CrossMark

JFM PAPERS

A Hamiltonian Dysthe equation for deep-water gravity waves with constant vorticity

Philippe Guyenne[1], Adilbek Kairzhan[2],†, and Catherine Sulem[2]

[1]Department of Mathematical Sciences, University of Delaware, Newark, DE 19716, USA

[2]Department of Mathematics, University of Toronto, Toronto, ON M5S2E4, Canada

This paper is a study of the water wave problem in a two-dimensional domain of infinite depth in the presence of non-zero constant vorticity. A goal is to describe the effects of uniform shear flow on the modulation of weakly nonlinear quasi-monochromatic surface gravity waves. Starting from the Hamiltonian formulation of this problem and using techniques from Hamiltonian transformation theory, we derive a Hamiltonian Dysthe equation for the time evolution of the wave envelope. Consistent with previous studies, we observe that the uniform shear flow tends to enhance or weaken the modulational instability of Stokes waves depending on its direction and strength. Our method also provides a non-perturbative procedure to reconstruct the surface elevation from the wave envelope, based on the Birkhoff normal form transformation to eliminate all non-resonant triads. This model is tested against direct numerical simulations of the full Euler equations and against a related Dysthe equation derived recently by Curtis, Carter & Kalisch (*J. Fluid Mech.*, vol. 855, 2018, pp. 322–350) in the context of constant vorticity. Very good agreement is found for a range of values of the vorticity.

1. Introduction

The water wave problem refers to the motion of a free surface over a body of water of finite or infinite depth. Its classical formulation usually assumes that the fluid is inviscid and irrotational. It is well known since the seminal work of Zakharov (1968) that in this setting, the water wave equations can be written as a Hamiltonian system with a standard Darboux symplectic structure whose Hamiltonian is the total energy. The canonical conjugate variables are given by (η, ξ), where $\eta(x, t)$ is the surface elevation, and $\xi(x, t)$ denotes the boundary values of the velocity potential on the free surface. With introduction of the Dirichlet–Neumann operator $G(\eta)$ that maps the Dirichlet boundary

† Email address for correspondence: kairzhan@math.toronto.edu

condition for a harmonic function in the fluid domain to its Neumann boundary condition, this Hamiltonian takes an explicit lower-dimensional form

$$H(\eta, \xi) = \frac{1}{2} \int_{\mathbb{R}} \left[\xi \, G(\eta) \, \xi + g\eta^2 \right] \mathrm{d}x, \tag{1.1}$$

in terms of surface variables alone (Craig & Sulem 1993). Moreover, the operator $G(\eta)$ is analytic with respect to η for Lipschitz functions η, and this provides an expansion of the Hamiltonian near the stationary solution $w = (\eta, \xi) = 0$, which corresponds to a fluid at rest (Coifman & Meyer 1985). The solution $w = 0$ is an elliptic stationary point in dynamical systems terms. In this Hamiltonian framework, perturbation calculations can be performed following general rules from Hamiltonian transformation theory, including canonical transformations and reduction to normal forms, to derive asymptotic models for weakly nonlinear water waves while preserving the Hamiltonian character of the original system (see Craig, Guyenne & Sulem (2021b) for a review).

Recently, a number of theoretical investigations have been devoted to the water wave problem with non-zero vorticity due to its relevance to oceanography and coastal engineering, where the influence of currents on waves may play an important role (Constantin 2001; Steer *et al.* 2019). Unlike the irrotational case, a full-dimensional computation is in general required to solve for the vorticity field. This has prompted efforts to propose simplified models for rotational waves in the long-wave shallow-water regime (Castro & Lannes 2014; Richard & Gavrilyuk 2015). Of special interest is the case of non-zero constant vorticity, which corresponds to vertically shear flow with a linear profile. The direction of the underlying current can be that of wave propagation (co-propagating) or opposite (counter-propagating). Similar to the irrotational water wave problem, this particular case allows for a lower-dimensional reformulation of the governing equations. As a consequence, it has received much attention in both mathematical and numerical studies, regarding e.g. the existence and stability of steadily progressing wave solutions (Teles Da Silva & Peregrine 1988; Vanden-Broeck 1996; Segal *et al.* 2017; Dyachenko & Hur 2019; Hur & Wheeler 2020; Blyth & Pǎrǎu 2022), the flow structure beneath waves (Ribeiro, Milewski & Nachbin 2017), or the focusing of transient waves by an adverse current (Choi 2009; Moreira & Chacaltana 2015).

Furthermore, as an extension of Zakharov's idea, a Hamiltonian formulation for nonlinear water waves with constant vorticity has been derived by Wahlén (2007) (see also Constantin, Ivanov & Prodanov 2008). The associated symplectic structure in terms of (η, ξ) is not canonical, but a change of variables reduces the system to a canonical one. Based on this formulation, recent work has been conducted involving long-wave modelling in the Korteweg–de Vries regime (Wahlén 2008), rigorous mathematical analysis on the existence of quasi-periodic travelling wave solutions (Berti, Franzoi & Maspero 2021), and direct numerical simulation of unsteady waves on deep or shallow water (Guyenne 2017, 2018). In particular, the reduction to surface variables makes it possible to solve the full equations via efficient and accurate numerical solvers such as the boundary integral method, the conformal mapping technique or the high-order spectral method.

This paper is devoted to the effects of constant vorticity in the setting of weakly nonlinear surface gravity waves, for which modulation theory is a classical tool. Under consideration is the asymptotic scaling regime where approximate solutions are constructed as slow modulations of monochromatic waves in two space dimensions. For this problem, Thomas, Kharif & Manna (2012) derived a cubic nonlinear Schrödinger (NLS) equation governing the envelope of surface gravity waves on finite depth using the method of multiple scales. Their analysis was extended to gravity–capillary waves by

Hsu *et al.* (2018), and to hydroelastic waves by Gao, Wang & Milewski (2019). Similarly, Curtis, Carter & Kalisch (2018) carried out the perturbation calculations up to an order higher, and obtained a Dysthe equation for gravity–capillary waves with constant vorticity on infinite depth. We also point out the earlier work of Baumstein (1998), who proposed an NLS equation for gravity waves in the presence of linear shear confined to a finite-depth layer near the free surface.

The classical theory for modulational analysis that describes the long-time evolution and stability of fast oscillatory solutions of nonlinear dispersive partial differential equations (PDEs) is based on the so-called modulational ansatz for solutions in the form of a weakly nonlinear narrowband wave train. In the context of gravity water waves, the leading non-trivial terms give rise to the NLS equation for the evolution of the slowly varying wave envelope (see Zakharov (1968) for the original derivation in the irrotational case). Dysthe (1979) later proposed a higher-order approximation for waves on deep water, which has since been extended to many other settings. The Dysthe equation and its variants are widely used in the oceanographic community because of their efficiency and ability to describe waves of moderately large steepness. It has been observed that numerical solutions of the Dysthe model provide a better agreement with laboratory experiments than the NLS equation, and are able e.g. to emulate the asymmetry of propagating wave packets, a feature not captured by the NLS equation (Lo & Mei 1985; Guyenne *et al.* 2021).

Unlike the NLS equation, which is a canonical Hamiltonian PDE, earlier versions of the Dysthe equation do not preserve the Hamiltonian character of the primitive equations. Gramstad & Trulsen (2011) used a Zakharov four-wave interaction model obtained by Krasitskii (1994) to derive a Hamiltonian version of Dysthe's equation for three-dimensional gravity waves on finite depth. Craig, Guyenne & Sulem (2021*a*) and Guyenne, Kairzhan & Sulem (2022) considered the modulational regimes for the two- and three-dimensional problems of gravity waves on deep water, respectively, and derived the corresponding Dysthe equations directly from the Euler equations for potential flow through a sequence of canonical transformations. By construction, the resulting Dysthe equations preserve the Hamiltonian character of the original problem. The main objective of the present paper is to extend this approach to the modulation of weakly nonlinear wave trains in the presence of constant vorticity, and derive a Dysthe equation that conforms with the Hamiltonian nature of the water wave system in this setting. We focus on the two-dimensional problem of wave propagation over infinite depth.

From a modelling viewpoint, it is desirable that such important structural properties as energy conservation are inherited by the approximation. Aside from interest in the Dysthe equation as an asymptotic model for water wave applications, this question is particularly relevant considering the successful and widespread use of the Hamiltonian formalism in physical sciences, including the field of fluid mechanics and free-surface flows (Benjamin & Olver 1982; Krasitskii 1994). The associated mathematical tools as applied to this physical problem are thus also of interest. Throughout our derivation, care is taken to perform both the expansion of the Hamiltonian functional and the canonical change of symplectic structure in a systematic manner, starting from the basic formulation introduced by Wahlén (2007). Our calculations are facilitated by the fact that the Dirichlet–Neumann operator admits an explicit Taylor series expansion (Craig & Sulem 1993). This property has been used extensively in previous studies on irrotational water waves (Lannes 2013), and can also be exploited here.

In modulation theory, reliance on a modulational ansatz implies that an additional step is required to reconstruct physical quantities such as the surface elevation from the solution of the envelope equation. This step is determined as part of the asymptotic analysis, and

in classical approaches like the method of multiple scales, this reconstruction is typically carried out perturbatively via a Stokes-type expansion. It is an important computation that also influences the model's performance, as shown e.g. in comparisons with experimental data on extreme waves (Zhang, Guedes Soares & Onorato 2015). In the present context, the reconstruction procedure is associated with the Birkhoff normal form transformation to eliminate all non-resonant triads. It is a non-perturbative computation but requires solving an auxiliary system of PDEs for the surface variables. In this way, higher-order harmonic contributions to the wave spectrum are generated automatically from the carrier wave component through nonlinear interactions according to these PDEs. We provide a detailed derivation of this auxiliary system for non-zero constant vorticity, noting that the resulting equations are significantly more complicated than in the irrotational case. By definition, these equations also take the form of a Hamiltonian evolutionary system with a canonical symplectic structure. As a consequence, the entire solution process fits within a Hamiltonian framework. Based on this approximation, we conduct a linear stability analysis and examine the dependence on vorticity. We then test analytical and numerical predictions from our model against direct numerical simulations of the full system, by inspecting the time evolution of perturbed Stokes waves and their possible instability. We also compare our results to numerical solutions of the related Dysthe model by Curtis *et al.* (2018), and discuss the performance of the different reconstruction methods. Previous observations on the focusing (resp. defocusing) effects of negative (resp. positive) vorticity associated with a counter-propagating (resp. co-propagating) current are recovered.

The starting point of our approach is the water wave system in its Hamiltonian canonical form in terms of the surface elevation and a modified velocity potential. In § 2, the Taylor expansion of the Hamiltonian is presented and then expressed in terms of the complex symplectic coordinates that diagonalize its quadratic terms. Unlike the irrotational case, the linear dispersion relation is not an even function of wavenumber. In § 3, we introduce elements of transformation theory and Birkhoff normal form transformations. A third-order Birkhoff normal form transformation that eliminates all non-resonant cubic terms from the Hamiltonian is calculated explicitly. It is defined as an auxiliary Hamiltonian flow from the original variables to transformed variables. In § 4, we propose the new Hamiltonian truncated at fourth order, and in § 5, we use the modulational ansatz together with a homogenization technique to derive the resonant quartic contributions. In § 6, the Hamiltonian Dysthe equation is obtained for the wave envelope. Section 7 is devoted to a validation of our approximation through numerical simulation and comparison with other models. First, a theoretical prediction on modulational stability of Stokes waves in the presence of constant vorticity is established. We then explain the procedure to reconstruct the surface variables by inverting the third-order Birkhoff normal form transformation, and we describe the numerical methods to solve the equations involved in the various models. Finally, we present a numerical investigation where predictions from our Hamiltonian Dysthe equation are compared to those from the envelope model by Curtis *et al.* (2018) and to direct simulations of the full water wave system.

2. The water wave system

2.1. *Governing equations*

We consider the evolution of a free surface $\{y = \eta(x, t)\}$ on top of a two-dimensional fluid of infinite depth

$$\mathcal{S}(\eta) = \{x \in \mathbb{R}, -\infty < y < \eta(x, t)\}, \tag{2.1}$$

under the influence of gravity. Assuming that the flow is incompressible and inviscid, the velocity field, denoted by $\boldsymbol{u}(x, y, t) = (u(x, y, t), v(x, y, t))^{\mathrm{T}}$, satisfies the Euler equations

$$\left.\begin{aligned} \partial_t \boldsymbol{u} + (\boldsymbol{u} \cdot \nabla)\boldsymbol{u} + \frac{1}{\rho}\nabla P - \boldsymbol{g} &= \boldsymbol{0}, \\ \nabla \cdot \boldsymbol{u} &= 0, \end{aligned}\right\} \tag{2.2}$$

where ρ is the (constant) fluid density, $P(x, y, t)$ is the pressure, and $\boldsymbol{g} = (0, -g)^{\mathrm{T}}$ is the acceleration due to gravity. Hereafter, the symbol ∇ denotes the spatial gradient $(\partial_x, \partial_y)^{\mathrm{T}}$ when applied to functions, or the variational gradient when applied to functionals. The vorticity, defined as

$$\gamma = \partial_x v - \partial_y u, \tag{2.3}$$

satisfies

$$\partial_t \gamma + (\boldsymbol{u} \cdot \nabla)\gamma = 0, \tag{2.4}$$

which expresses the well-known fact that in two dimensions, the vorticity is conserved along particle trajectories. In particular, if the initial vorticity is constant throughout the fluid domain, then it remains constant. The present study is devoted to flows with the property of having non-zero constant vorticity.

The boundary conditions at the free surface are composed of the dynamical condition

$$P = P_0, \tag{2.5}$$

where P_0 is the atmospheric constant, and the kinematic condition

$$v = \partial_t \eta + u \, \partial_x \eta. \tag{2.6}$$

The divergence-free condition implies the existence of a stream function ψ such that

$$u = \partial_y \psi, \quad v = -\partial_x \psi, \tag{2.7a,b}$$

satisfying

$$-\Delta \psi = \gamma. \tag{2.8}$$

By construction, $\tilde{\psi} = \psi + \gamma y^2/2$ is a harmonic function. Introducing the generalized potential φ, defined as the harmonic conjugate of $\tilde{\psi}$, we have

$$\left.\begin{aligned} \partial_x \varphi = \partial_y \tilde{\psi} &= u + \gamma y, \\ \partial_y \varphi = -\partial_x \tilde{\psi} &= v. \end{aligned}\right\} \tag{2.9}$$

The presence of constant vorticity induces a horizontal background shear current that has a linear profile in the vertical direction. We associate $\gamma > 0$ with a co-propagating current because it contributes positively to the horizontal fluid velocity $u = \partial_x \varphi - \gamma y$ for $y < 0$ (along most of the water column), while $\gamma < 0$ is associated with a counter-propagating current.

In the variables φ and $\tilde{\psi}$, (2.2) takes the form

$$\nabla \left[\partial_t \varphi + \tfrac{1}{2} \left((\partial_x \varphi)^2 + (\partial_y \varphi)^2 \right) + \gamma \tilde{\psi} - \gamma y \, \partial_x \varphi + P + gy \right] = \mathbf{0}, \qquad (2.10)$$

and after integration, it reduces to

$$\partial_t \varphi + \tfrac{1}{2} \left((\partial_x \varphi)^2 + (\partial_y \varphi)^2 \right) + \gamma \tilde{\psi} - \gamma \eta \, \partial_x \varphi + g\eta = 0, \qquad (2.11)$$

at the free surface $y = \eta$, with $P_0 = 0$ without loss of generality. The Euler system can then be written as

$$\Delta \varphi = 0 \quad \text{in } \mathcal{S}, \qquad (2.12)$$

$$\partial_t \eta - \partial_y \varphi + (\partial_x \varphi)(\partial_x \eta) - \gamma \eta \, \partial_x \eta = 0, \quad \text{on } y = \eta(x, t), \qquad (2.13)$$

$$\partial_t \varphi + \tfrac{1}{2} \left((\partial_x \varphi)^2 + (\partial_y \varphi)^2 \right) + \gamma \tilde{\psi} - \gamma \eta \, \partial_x \varphi + g\eta = 0, \quad \text{on } y = \eta(x, t), \qquad (2.14)$$

with the condition that $\varphi, \tilde{\psi} \to 0$ uniformly in x as $y \to -\infty$.

2.2. *Hamiltonian formulation*

It is well known since the seminal paper of Zakharov (1968) that the irrotational ($\gamma = 0$) water wave system has a Hamiltonian formulation in the variables (η, ξ), where $\xi(x, t) = \varphi(x, \eta(x, t), t)$ is the trace of the velocity potential on the free surface.

Wahlén (2007) (see also Constantin *et al.* 2008) observed that in the presence of constant vorticity, the water wave system in (η, ξ) can still be expressed as a Hamiltonian system but in non-canonical form, namely

$$\partial_t \begin{pmatrix} \eta \\ \xi \end{pmatrix} = \begin{pmatrix} 0 & 1 \\ -1 & \gamma \, \partial_x^{-1} \end{pmatrix} \begin{pmatrix} \partial_\eta H \\ \partial_\xi H \end{pmatrix}. \qquad (2.15)$$

The Hamiltonian $H(\eta, \xi)$ is the total energy:

$$H(\eta, \xi) = \frac{1}{2} \int_{\mathbb{R}} \left[\xi \, G(\eta) \, \xi - \gamma \eta^2 \, \partial_x \xi + \frac{\gamma^2}{3} \eta^3 + g\eta^2 \right] \mathrm{d}x, \qquad (2.16)$$

where $G(\eta)$ is the Dirichlet–Neumann operator in the fluid domain, which associates to the Dirichlet data ξ on $y = \eta(x)$ the normal derivative of the harmonic function φ with an additional normalized factor, namely

$$G(\eta) : \xi \longmapsto \sqrt{1 + (\partial_x \eta)^2} \, \partial_n \varphi \big|_{y=\eta}. \qquad (2.17)$$

Other invariants of motion are the volume (or mass)

$$V = \int_{\mathbb{R}} \eta \, \mathrm{d}x, \qquad (2.18)$$

and the momentum (or impulse)

$$I = \int_{\mathbb{R}} \left(\eta \, \partial_x \xi - \tfrac{1}{2} \gamma \eta^2 \right) \mathrm{d}x. \qquad (2.19)$$

Wahlén (2007) found that under the change of variables

$$(\eta, \xi) \to \left(\eta, \zeta = \xi - \frac{\gamma}{2} \partial_x^{-1} \eta \right), \qquad (2.20)$$

system (2.15) can be transformed into canonical form

$$\partial_t \begin{pmatrix} \eta \\ \zeta \end{pmatrix} = J \nabla \mathcal{H}(\eta, \zeta) = \begin{pmatrix} 0 & 1 \\ -1 & 0 \end{pmatrix} \begin{pmatrix} \partial_\eta \mathcal{H} \\ \partial_\zeta \mathcal{H} \end{pmatrix}, \tag{2.21}$$

where the Hamiltonian $\mathcal{H}(\eta, \zeta) = H(\eta, \xi)$ in the new variables is

$$\mathcal{H}(\eta, \zeta) = \frac{1}{2} \int_{\mathbb{R}} \left[\left(\zeta + \frac{\gamma}{2} \partial_x^{-1} \eta \right) G(\eta) \left(\zeta + \frac{\gamma}{2} \partial_x^{-1} \eta \right) - \gamma \eta^2 \partial_x \zeta - \frac{\gamma^2}{6} \eta^3 + g \eta^2 \right] dx. \tag{2.22}$$

In the above formulas, $\partial_x^{-1} \eta$ is defined as $\partial_x^{-1} \eta(x) = \int_{-\infty}^x \eta(s) \, ds$. We assume that $\eta \to 0$ as $x \to \pm\infty$. Furthermore, we assume that $\int_{-\infty}^{\infty} \eta \, dx = 0$ at $t = 0$, which implies that it remains so for all t. Indeed, integrating (2.13) in x over $\mathbb{R}$, we get

$$\partial_t \int_{\mathbb{R}} \eta \, dx - \int_{\mathbb{R}} \left(G(\eta) \xi - \frac{\gamma}{2} \partial_x \eta^2 \right) dx = 0. \tag{2.23}$$

The second term on the left-hand side rewrites as $\int_{\mathbb{R}} G(\eta) \xi \, dx = \int_{\partial S} \partial_n \varphi \, d\sigma = \int_S \Delta \varphi \, dx \, dy = 0$, leading to $\int_{\mathbb{R}} \eta \, dx = 0$ for all t.

Denoting by $\hat{f}_k = (1/\sqrt{2\pi}) \int_{\mathbb{R}} e^{-ikx} f(x) \, dx$ the Fourier transform of a function $f(x)$, we have in particular

$$\partial_x^{-1} \eta(x) = -\frac{i}{\sqrt{2\pi}} \int_{\mathbb{R}} \frac{1}{k} \hat{\eta}_k \, e^{ikx} \, dk, \quad \partial_x \zeta(x) = \frac{i}{\sqrt{2\pi}} \int_{\mathbb{R}} k \hat{\zeta}_k \, e^{ikx} \, dk. \tag{2.24a,b}$$

From the above assumption,

$$\hat{\eta}_0 = 0, \quad \hat{\eta}_k = O(k) \text{ for small } k. \tag{2.25}$$

In the following, we will drop the hat notation. Since $\eta(x)$ and $\zeta(x)$ are real-valued functions, we have the relation $(\eta_{-k}, \zeta_{-k}) = (\bar{\eta}_k, \bar{\zeta}_k)$ where the overbar stands for complex conjugation.

2.3. *Taylor expansion of the Hamiltonian near equilibrium*

It can be shown that the Dirichlet–Neumann operator is analytic in η (Coifman & Meyer 1985) and admits a convergent Taylor series expansion

$$G(\eta) = \sum_{m=0}^{\infty} G^{(m)}(\eta) \tag{2.26}$$

about the quiescent state $\eta = 0$. For each m, the term $G^{(m)}(\eta)$ is homogeneous of degree m in η, and can be calculated explicitly via recursive relations (Craig & Sulem 1993).

Denoting $D = -\mathrm{i}\,\partial_x$, the first three terms are

$$
\left.
\begin{aligned}
G^{(0)}(\eta) &= |D|, \\
G^{(1)}(\eta) &= D\eta D - G^{(0)}\eta G^{(0)}, \\
G^{(2)}(\eta) &= -\frac{1}{2}\left(|D|^2\eta^2 G^{(0)} + G^{(0)}\eta^2|D|^2 - 2G^{(0)}\eta G^{(0)}\eta G^{(0)}\right).
\end{aligned}
\right\}
\tag{2.27}
$$

In Fourier variables, substituting the expansion for $G(\eta)$ into the Hamiltonian (2.22), we get

$$
\mathcal{H} = \mathcal{H}^{(2)} + \mathcal{H}^{(3)} + \mathcal{H}^{(4)} + \cdots,
\tag{2.28}
$$

where each term $\mathcal{H}^{(m)}$ is homogeneous of degree m in (η, ζ). In particular, we have

$$
\left.
\begin{aligned}
\mathcal{H}^{(2)} &= \frac{1}{2}\int_{\mathbb{R}}\left[|k|\left(\zeta_k - \frac{\mathrm{i}\gamma}{2k}\,\eta_k\right)\left(\bar{\zeta}_k + \frac{\mathrm{i}\gamma}{2k}\,\bar{\eta}_k\right) + g|\eta_k|^2\right]\mathrm{d}k, \\
\mathcal{H}^{(3)} &= \frac{1}{2\sqrt{2\pi}}\int_{\mathbb{R}^3}\left[(-k_1 k_3 - |k_1|\,|k_3|)\left(\zeta_1 - \frac{\mathrm{i}\gamma}{2k_1}\,\eta_1\right)\eta_2\left(\zeta_3 - \frac{\mathrm{i}\gamma}{2k_3}\,\eta_3\right)\right. \\
&\qquad\left. -\mathrm{i}\gamma k_1\zeta_1\eta_2\eta_3 - \frac{\gamma^2}{6}\,\eta_1\eta_2\eta_3\right]\delta_{123}\,\mathrm{d}k_{123}, \\
\mathcal{H}^{(4)} &= -\frac{1}{8\pi}\int_{\mathbb{R}^4}|k_1|\,|k_4|\,(|k_1| + |k_4| - 2|k_3 + k_4|)\left(\zeta_1 - \frac{\mathrm{i}\gamma}{2k_1}\,\eta_1\right)\eta_2\eta_3 \\
&\qquad\times\left(\zeta_4 - \frac{\mathrm{i}\gamma}{2k_4}\,\eta_4\right)\delta_{1234}\,\mathrm{d}k_{1234}.
\end{aligned}
\right\}
\tag{2.29}
$$

In the above expressions, we use the compact notations $(\eta_j, \zeta_j) = (\eta_{k_j}, \zeta_{k_j})$, $\mathrm{d}k_{1\ldots n} = \mathrm{d}k_1\ldots\mathrm{d}k_n$ and $\delta_{1\ldots n} = \delta(k_1 + \cdots + k_n)$, where $\delta(k) = (1/2\pi)\int_{\mathbb{R}}\mathrm{e}^{-\mathrm{i}kx}\,\mathrm{d}x$ is the Dirac distribution. Hereafter, the domain of integration is omitted in integrals and is understood to be $\mathbb{R}$ for each x_j or k_j.

2.4. *Linearization near equilibrium*

The linearized water wave system about still water, written in terms of (η, ζ), is

$$
\partial_t\begin{pmatrix}\eta \\ \zeta\end{pmatrix} = J\,\nabla\mathcal{H}^{(2)}(\eta, \zeta) = \begin{pmatrix} g - \dfrac{\gamma^2}{4}\,\partial_x^{-1}|D|\,\partial_x^{-1} & -\dfrac{\gamma}{2}\,\partial_x^{-1}|D| \\[2mm] \dfrac{\gamma}{2}\,\partial_x^{-1}|D| & |D| \end{pmatrix}\begin{pmatrix}\eta \\ \zeta\end{pmatrix}.
\tag{2.30}
$$

We now introduce the symplectic complex coordinate

$$
z := \frac{1}{\sqrt{2}}\left(a(D)\,\eta + \mathrm{i}\,a(D)^{-1}\,\zeta\right),
\tag{2.31}
$$

where $a^2(D) := \omega(D)/|D|$, and $\omega(D) := \sqrt{\gamma^2/4 + g\,|D|}$. The mapping $(\eta, \zeta) \to (z, \bar{z})$ is canonical, and in these variables, the water wave system becomes

$$
\partial_t\begin{pmatrix}z \\ \bar{z}\end{pmatrix} = \begin{pmatrix}0 & -\mathrm{i} \\ \mathrm{i} & 0\end{pmatrix}\begin{pmatrix}\partial_z\mathcal{H} \\ \partial_{\bar{z}}\mathcal{H}\end{pmatrix} := J_1\begin{pmatrix}\partial_z\mathcal{H} \\ \partial_{\bar{z}}\mathcal{H}\end{pmatrix}.
\tag{2.32}
$$

Equivalently, in the Fourier space,

$$z_k := \frac{1}{\sqrt{2}} \left(a_k \eta_k + i\, a_k^{-1} \zeta_k \right), \tag{2.33}$$

where $a_k^2 = \omega_k/|k|$ and $\omega_k = \sqrt{\gamma^2/4 + g\,|k|}$. Since the functions $\eta(x)$ and $\zeta(x)$ are real-valued in the physical space, we also have

$$\bar{z}_{-k} = \frac{1}{\sqrt{2}} \left(a_k \eta_k - i\, a_k^{-1} \zeta_k \right). \tag{2.34}$$

We can express η_k and ζ_k in terms of z_k as

$$\eta_k = \frac{1}{\sqrt{2}} a_k^{-1}(z_k + \bar{z}_{-k}), \quad \zeta_k = \frac{1}{i\sqrt{2}} a_k(z_k - \bar{z}_{-k}). \tag{2.35a,b}$$

The quadratic term $\mathcal{H}^{(2)}$ given in (2.29) diagonalizes as

$$\mathcal{H}^{(2)} = \int \Omega_k\, |z_k|^2 \,\mathrm{d}k, \tag{2.36}$$

where

$$\Omega_k = \Omega(k) = \frac{\gamma}{2}\,\mathrm{sgn}(k) + \omega_k \tag{2.37}$$

is the linear dispersion relation for deep-water gravity waves with constant vorticity (Berti *et al.* 2021). The linearized system with $\mathcal{H}$ replaced by $\mathcal{H}^{(2)}$ in (2.32) reduces to the scalar equation $\partial_t z_k = -i\,\Omega_k z_k$.

We define the Poisson bracket of two functionals $K(\eta, \zeta)$ and $H(\eta, \zeta)$ of real-valued functions η and ζ as

$$\{K, H\} = \int \left(\partial_\eta H\, \partial_\zeta K - \partial_\zeta H\, \partial_\eta K \right) \mathrm{d}x. \tag{2.38}$$

Assuming that K and H are real-valued, and using the Plancherel formula, it is written in terms of the Fourier variables as

$$\{K, H\} = \int \left(\partial_{\eta_k} H\, \overline{\partial_{\zeta_k} K} - \partial_{\zeta_k} H\, \overline{\partial_{\eta_k} K} \right) \mathrm{d}k = \int \left(\partial_{\eta_k} H\, \partial_{\bar{\zeta}_k} K - \partial_{\zeta_k} H\, \partial_{\bar{\eta}_k} K \right) \mathrm{d}k$$

$$= \int \left(\partial_{\eta_k} H\, \delta_{\zeta_{-k}} K - \partial_{\zeta_k} H \partial_{\eta_{-k}} K \right) \mathrm{d}k = \int \left(\partial_{\eta_{k_1}} H\, \partial_{\zeta_{k_2}} K - \partial_{\zeta_{k_1}} H\, \partial_{\eta_{k_2}} K \right) \delta_{12} \,\mathrm{d}k_{12}. \tag{2.39}$$

In terms of the complex symplectic coordinates, it becomes

$$\{K, H\} = \frac{1}{i} \int (\partial_{z_{k_1}} H\, \partial_{\bar{z}_{-k_2}} K - \partial_{\bar{z}_{-k_1}} H\, \partial_{z_{k_2}} K)\, \delta_{12} \,\mathrm{d}k_{12}. \tag{2.40}$$

3. Birkhoff normal form transformations

3.1. *Third-order term in the Hamiltonian*

The cubic term $\mathcal{H}^{(3)}$ given in (2.29) can be simplified further due to symmetries. We first state a simple identity that will be useful throughout the paper.

LEMMA 3.1. *For any* $(k_1, k_2, k_3) \in \mathbb{R}^3$ *with* $k_1 + k_2 + k_3 = 0$ *and* $k_j \neq 0$, *we have*

$$\text{sgn}(k_1)\,\text{sgn}(k_2) + \text{sgn}(k_1)\,\text{sgn}(k_3) + \text{sgn}(k_2)\,\text{sgn}(k_3) = -1. \tag{3.1}$$

Proof. Consider the different sectors of the (k_1, k_2)-plane, and check that the equality is satisfied in each sector. ∎

LEMMA 3.2. *The cubic term* $\mathcal{H}^{(3)}$ *in* (2.29) *can be written as*

$$\mathcal{H}^{(3)} = -\frac{1}{2\sqrt{2\pi}} \int (1 + \text{sgn}(k_1)\,\text{sgn}(k_3)) \left(|k_1|\,|k_3|\,\zeta_1\eta_2\zeta_3 + \mathrm{i}\,\frac{\gamma k_2}{2}\,\eta_1\zeta_2\eta_3 \right) \delta_{123}\, \mathrm{d}k_{123}. \tag{3.2}$$

Proof. Expanding the brackets in (2.29), we regroup the terms as follows:

$$\mathcal{H}^{(3)} = \frac{1}{2\sqrt{2\pi}} \int \left[(-k_1k_3 - |k_1|\,|k_3|)\zeta_1\eta_2\zeta_3 + (k_1k_3 + |k_1|\,|k_3|)\,\frac{\mathrm{i}\gamma}{k_1}\,\eta_1\eta_2\zeta_3 - \mathrm{i}\gamma k_1\zeta_1\eta_2\eta_3 \right. $$
$$\left. + \left((k_1k_3 + |k_1|\,|k_3|)\,\frac{\gamma^2}{4k_1k_3} - \frac{\gamma^2}{6} \right) \eta_1\eta_2\eta_3 \right] \delta_{123}\, \mathrm{d}k_{123}. \tag{3.3}$$

The term on the second line of (3.3) corresponding to $\eta_1\eta_2\eta_3$ vanishes because of the symmetry in $\eta_1\eta_2\eta_3$ under index rearrangements, and identity (3.1). Indeed, we have

$$\int (k_1k_3 + |k_1|\,|k_3|)\,\frac{\gamma^2}{4k_1k_3}\,\eta_1\eta_2\eta_3\,\delta_{123}\, \mathrm{d}k_{123} = \frac{\gamma^2}{4} \int (1 + \text{sgn}(k_1)\,\text{sgn}(k_3))\eta_1\eta_2\eta_3\,\delta_{123}\, \mathrm{d}k_{123}$$
$$= \frac{\gamma^2}{6} \int \eta_1\eta_2\eta_3\,\delta_{123}\, \mathrm{d}k_{123}. \tag{3.4}$$

As a result, $\mathcal{H}^{(3)}$ simplifies to

$$\mathcal{H}^{(3)} = -\frac{1}{2\sqrt{2\pi}} \int \left[(1 + \text{sgn}(k_1)\,\text{sgn}(k_3))\,|k_1|\,|k_3|\,\zeta_1\eta_2\zeta_3 \right.$$
$$\left. -\mathrm{i}\gamma\,|k_1|\,\text{sgn}(k_3)\,\zeta_1\eta_2\eta_3 \right] \delta_{123}\, \mathrm{d}k_{123}. \tag{3.5}$$

The first term in (3.5) identifies to the first term in (3.2), while its second term can be transformed using index rearrangements and identity (3.1) as follows:

$$\int |k_1|\,\text{sgn}(k_3)\,\zeta_1\eta_2\eta_3\,\delta_{123}\, \mathrm{d}k_{123} = \int |k_2|\,\text{sgn}(k_3)\,\eta_1\zeta_2\eta_3\,\delta_{123}\, \mathrm{d}k_{123}$$
$$= \int \frac{|k_2|}{2}\,(\text{sgn}(k_1) + \text{sgn}(k_3))\eta_1\zeta_2\eta_3\,\delta_{123}\, \mathrm{d}k_{123}$$
$$= -\int \frac{k_2}{2}\,(1 + \text{sgn}(k_1)\,\text{sgn}(k_3))\,\eta_1\zeta_2\eta_3\,\delta_{123}\, \mathrm{d}k_{123}. \tag{3.6}$$

∎

In terms of the complex symplectic coordinates, $\mathcal{H}^{(3)}$ is a linear combination of third-order monomials:

$$\mathcal{H}^{(3)} = \frac{1}{8\sqrt{\pi}} \int \frac{1 + \text{sgn}(k_1)\,\text{sgn}(k_3)}{a_1 a_2 a_3} \left(\omega_1\omega_3 - \frac{\gamma\omega_2}{2}\,\text{sgn}(k_2) \right)$$
$$\times (z_1 z_2 z_3 + \bar{z}_1\bar{z}_2\bar{z}_3 - 2(\bar{z}_{-1}\bar{z}_{-2}z_3 + z_{-1}z_{-2}\bar{z}_3) + \bar{z}_{-1}z_2\bar{z}_{-3} + z_{-1}\bar{z}_2 z_{-3})\,\delta_{123}\, \mathrm{d}k_{123}. \tag{3.7}$$

949 A50-10

3.2. *Canonical transformations*

We are looking for a canonical transformation of the physical variables

$$\tau : w = \begin{pmatrix} \eta \\ \zeta \end{pmatrix} \longmapsto w', \tag{3.8}$$

defined in a neighbourhood of the origin, such that the transformed Hamiltonian $\mathcal{H}'$ satisfies

$$\mathcal{H}'(w') = \mathcal{H}(\tau^{-1}(w')), \quad \partial_t w' = J \nabla \mathcal{H}'(w'), \tag{3.9a,b}$$

and reduces to

$$\mathcal{H}'(w') = \mathcal{H}^{(2)}(w') + Z^{(4)} + Z^{(5)} + \cdots, \tag{3.10}$$

where each term $Z^{(m)}$ is of degree m, and all cubic terms are eliminated. We construct the transformation τ by the Lie transform method as a Hamiltonian flow ϕ from 'time' $s = -1$ to 'time' $s = 0$ governed by

$$\partial_s \phi = J \nabla K(\phi), \quad \phi(w')|_{s=0} = w', \quad \phi(w')|_{s=-1} = w, \tag{3.11a–c}$$

and associated to an auxiliary Hamiltonian K. Such a transformation is canonical and preserves the Hamiltonian structure of the system. The Hamiltonian $\mathcal{H}'$ satisfies $\mathcal{H}'(w') = \mathcal{H}(\phi(w'))|_{s=-1}$, and its Taylor expansion around $s = 0$ is

$$\mathcal{H}'(w') = \mathcal{H}(\phi(w'))|_{s=0} - \frac{d\mathcal{H}}{ds}(\phi(w'))|_{s=0} + \frac{1}{2} \frac{d^2\mathcal{H}}{ds^2}(\phi(w'))|_{s=0} - \cdots. \tag{3.12}$$

Abusing notation, we further use $w = (\eta, \zeta)^{\mathrm{T}}$ to denote the new variable w'. Terms in this expansion can be expressed using Poisson brackets as

$$\mathcal{H}(\phi(w))|_{s=0} = \mathcal{H}(w), \tag{3.13}$$

$$\frac{d\mathcal{H}}{ds}(\phi(w))|_{s=0} = \int \left(\partial_\eta \mathcal{H} \, \partial_s \eta + \partial_\zeta \mathcal{H} \, \partial_s \zeta \right) dx$$

$$= \int \left(\partial_\eta \mathcal{H} \, \partial_\zeta K - \partial_\zeta \mathcal{H} \, \partial_\eta K \right) dx = \{K, \mathcal{H}\}(w), \tag{3.14}$$

and similarly for the remaining terms. The Taylor expansion of $\mathcal{H}'$ around $s = 0$ now has the form

$$\mathcal{H}'(w) = \mathcal{H}(w) - \{K, \mathcal{H}\}(w) + \tfrac{1}{2} \{K, \{K, \mathcal{H}\}\}(w) - \cdots. \tag{3.15}$$

Substituting this transformation into the expansion (2.28) of H, we obtain

$$\mathcal{H}'(w) = \mathcal{H}^{(2)}(w) + \mathcal{H}^{(3)}(w) + \cdots$$
$$- \{K, \mathcal{H}^{(2)}\}(w) - \{K, \mathcal{H}^{(3)}\}(w) - \{K, \mathcal{H}^{(4)}\}(w) - \cdots$$
$$+ \tfrac{1}{2}\{K, \{K, \mathcal{H}^{(2)}\}\}(w) + \tfrac{1}{2} \{K, \{K, \mathcal{H}^{(3)}\}\}(w) + \cdots. \tag{3.16}$$

If K is homogeneous of degree m, and $\mathcal{H}^{(n)}$ is homogeneous of degree n, then $\{K, \mathcal{H}^{(n)}\}$ is of degree $m + n - 2$. Thus in order to get the Hamiltonian as in (3.10), we need to construct, if possible, an auxiliary Hamiltonian $K = K^{(3)}$ that is homogeneous of degree 3 and satisfies the relation

$$\mathcal{H}^{(3)} - \{K^{(3)}, \mathcal{H}^{(2)}\} = 0, \tag{3.17}$$

which would eliminate all cubic terms from the transformed Hamiltonian $\mathcal{H}'$. In the following, we will show that it is possible to do this, and that there are no resonant cubic terms in the Hamiltonian.

3.3. *Third-order Birkhoff normal form*

To find the auxiliary Hamiltonian $K^{(3)}$ from (3.17), we use the following diagonal property of the coadjoint operator $\mathrm{coad}_{\mathcal{H}^{(2)}} := \{\cdot, \mathcal{H}^{(2)}\}$ when applied to monomial terms (Craig & Sulem 2016). For example, taking $\mathcal{I} := \int z_1 z_2 \bar{z}_{-3}\, \delta_{123}\, \mathrm{d}k_{123}$, we have

$$\{\mathcal{I}, \mathcal{H}^{(2)}\} = \mathrm{i} \int (\Omega_1 + \Omega_2 - \Omega_{-3}) z_1 z_2 \bar{z}_{-3}\, \delta_{123}\, \mathrm{d}k_{123}, \tag{3.18}$$

where $\Omega_{\pm j} := \Omega_{\pm k_j}$.

PROPOSITION 3.1. *The cohomological equation* (3.17) *has a unique solution* $K^{(3)}$ *that in complex symplectic coordinates is*

$$K^{(3)} = \frac{1}{8\mathrm{i}\sqrt{\pi}} \int \frac{1 + \mathrm{sgn}(k_1)\,\mathrm{sgn}(k_3)}{a_1 a_2 a_3} \left(\omega_1 \omega_3 - \frac{\gamma \omega_2}{2}\,\mathrm{sgn}(k_2)\right) \delta_{123}$$
$$\times \left(\frac{z_1 z_2 z_3 - \bar{z}_1 \bar{z}_2 \bar{z}_3}{\Omega_1 + \Omega_2 + \Omega_3} + 2\frac{\bar{z}_{-1}\bar{z}_{-2} z_3 - z_{-1} z_{-2} \bar{z}_3}{\Omega_{-1} + \Omega_{-2} - \Omega_3} - \frac{\bar{z}_{-1} z_2 \bar{z}_{-3} - z_{-1} \bar{z}_2 z_{-3}}{\Omega_{-1} - \Omega_2 + \Omega_{-3}}\right) \mathrm{d}k_{123}. \tag{3.19}$$

Alternatively, in the (η, ζ) *variables,* $K^{(3)}$ *has the form*

$$K^{(3)} = \frac{1}{4\mathrm{i}\sqrt{2\pi}} \int (1 + \mathrm{sgn}(k_1)\,\mathrm{sgn}(k_3))\,\delta_{123}$$
$$\times \left[-\frac{\dfrac{\gamma^4}{8} + \dfrac{\gamma^2}{2} g\,|k_2| + g^2\,|k_1|\,|k_3|}{g^2\,|k_1|\,|k_3|} \right.$$
$$\left(-\frac{\gamma}{2}\,\mathrm{sgn}(k_2)\,\eta_1 \eta_2 \eta_3 + \mathrm{i}\,|k_2|\,\eta_1 \zeta_2 \eta_3 - 2\mathrm{i}\,|k_3|\,\eta_1 \eta_2 \zeta_3\right)$$
$$+ \frac{\gamma\,\mathrm{sgn}(k_2)}{g^2\,|k_1|\,|k_3|} \left(2\omega_3^2\,|k_1|\,|k_2|\,\zeta_1 \zeta_2 \eta_3 - \omega_2^2\,|k_1|\,|k_3|\,\zeta_1 \eta_2 \zeta_3\right.$$
$$\left.\left. + \mathrm{i}\frac{\gamma\,\mathrm{sgn}(k_2)}{2}\,|k_1|\,|k_2|\,|k_3|\,\zeta_1 \zeta_2 \zeta_3\right) \right] \mathrm{d}k_{123}. \tag{3.20}$$

Proof. Using (3.7) and diagonal properties of the coadjoint operator as in (3.18), we solve (3.17) uniquely for $K^{(3)}$, and derive (3.19).

To obtain (3.20), we first need to rewrite (3.19) as a linear combination of third-order terms in z_j and z_{-j} only ($j = 1, 2, 3$). This can be done by applying the change of indices $(k_1, k_2, k_3) \to (-k_1, -k_2, -k_3)$ to monomials $\bar{z}_1 \bar{z}_2 \bar{z}_3$, $z_{-1} z_{-2} \bar{z}_3$ and $z_{-1} \bar{z}_2 z_{-3}$. Then (3.20) is obtained in terms of (η_k, ζ_k) using (2.33) and (2.34). $\blacksquare$

REMARK 3.1. *The auxiliary Hamiltonian* $K^{(3)}$ *obtained in Proposition 3.1 is well-defined. There are no singularities due to the denominators* k_1, k_3 *since* $\eta_k = O(k)$ *as* $k \to 0$.

Below, we write an alternative representation of the auxiliary Hamiltonian $K^{(3)}$ that will be useful later when we compute the Poisson bracket $\{\mathcal{H}^{(3)}, K^{(3)}\}$. Introduce the coefficient functions

$$S_{123} := \frac{1 + \mathrm{sgn}(k_1)\,\mathrm{sgn}(k_3)}{a_1 a_2 a_3}\left(k_1 k_3 a_1^2 a_3^2 - \frac{\gamma}{2}\,k_2 a_2^2\right), \quad A_{123} := \frac{1}{8\sqrt{\pi}}\,(S_{123} + S_{312} - S_{231}).$$

$$(3.21a,b)$$

Note that $S_{123} = S_{321}$.

LEMMA 3.3. *We have*

$$\left.\begin{aligned}
\mathcal{H}^{(3)} &= \int A_{123}(z_1 z_2 z_3 + \bar{z}_1 \bar{z}_2 \bar{z}_3 - z_{-1} z_{-2} \bar{z}_3 - \bar{z}_{-1} \bar{z}_{-2} z_3)\,\delta_{123}\,\mathrm{d}k_{123}, \\
K^{(3)} &= \frac{1}{\mathrm{i}} \int \left[\frac{A_{123}(z_1 z_2 z_3 - \bar{z}_1 \bar{z}_2 \bar{z}_3)}{\Omega_1 + \Omega_2 + \Omega_3} - \frac{A_{123}(z_{-1} z_{-2} \bar{z}_3 - \bar{z}_{-1} \bar{z}_{-2} z_3)}{\Omega_{-1} + \Omega_{-2} - \Omega_3}\right]\delta_{123}\,\mathrm{d}k_{123}.
\end{aligned}\right\}$$

$$(3.22)$$

Proof. From (3.7), using that $k_1 k_3 = |k_1|\,|k_3|$ whenever $1 + \mathrm{sgn}(k_1)\,\mathrm{sgn}(k_3) \neq 0$, we have

$$\mathcal{H}^{(3)} = \frac{1}{8\sqrt{\pi}} \int S_{123}\,((z_1 z_2 z_3 + \bar{z}_1 \bar{z}_2 \bar{z}_3) - 2(z_{-1} z_{-2} \bar{z}_3 + \bar{z}_{-1} \bar{z}_{-2} z_3)$$
$$+ (\bar{z}_{-1} z_2 \bar{z}_{-3} + z_{-1} \bar{z}_2 z_{-3}))\,\delta_{123}\,\mathrm{d}k_{123}. \quad (3.23)$$

By symmetry, the first term on the right-hand side in (3.23) becomes

$$\frac{1}{8\sqrt{\pi}} \int S_{123}(z_1 z_2 z_3 + \bar{z}_1 \bar{z}_2 \bar{z}_3)\,\delta_{123}\,\mathrm{d}k_{123} = \int A_{123}(z_1 z_2 z_3 + \bar{z}_1 \bar{z}_2 \bar{z}_3)\,\delta_{123}\,\mathrm{d}k_{123}. \quad (3.24)$$

The second term in (3.23) has two copies of $(z_{-1} z_{-2} \bar{z}_3 + \bar{z}_{-1} \bar{z}_{-2} z_3)$. We keep one copy as it is, and apply two index rearrangements to the second copy. First, $(k_1, k_2, k_3) \rightarrow (k_3, k_2, k_1)$ gives

$$\int S_{123}(z_{-1} z_{-2} \bar{z}_3 + \bar{z}_{-1} \bar{z}_{-2} z_3)\,\delta_{123}\,\mathrm{d}k_{123} = \int S_{123}(\bar{z}_1 z_{-2} z_{-3} + z_1 \bar{z}_{-2} \bar{z}_{-3})\,\delta_{123}\,\mathrm{d}k_{123}, \quad (3.25)$$

where we use that $S_{123} = S_{321}$. Second, $(1, 2, 3) \rightarrow (3, 1, 2)$ implies

$$\int S_{123}(\bar{z}_1 z_{-2} z_{-3} + z_1 \bar{z}_{-2} \bar{z}_{-3})\,\delta_{123}\,\mathrm{d}k_{123} = \int S_{312}(z_{-1} z_{-2} \bar{z}_3 + \bar{z}_{-1} \bar{z}_{-2} z_3)\,\delta_{123}\,\mathrm{d}k_{123}. \quad (3.26)$$

For the third term in (3.23), we apply $(k_1, k_2, k_3) \rightarrow (k_2, k_3, k_1)$ and leave details to the reader. Combining all the transformations above, we obtain

$$\frac{1}{8\sqrt{\pi}} \int S_{123}\,(-2(z_{-1} z_{-2} \bar{z}_3 + \bar{z}_{-1} \bar{z}_{-2} z_3) + \bar{z}_{-1} z_2 \bar{z}_{-3} + z_{-1} \bar{z}_2 z_{-3})\,\delta_{123}\,\mathrm{d}k_{123}$$

$$= \int A_{123}(-z_{-1} z_{-2} \bar{z}_3 - \bar{z}_{-1} \bar{z}_{-2} z_3)\,\delta_{123}\,\mathrm{d}k_{123}, \quad (3.27)$$

which together with (3.24) implies the first relation of (3.22). The second equation in (3.22) is derived from (3.17) by using the diagonal properties (3.18). ∎

The third-order normal form transformation defining the new coordinates is obtained as the solution map at $s = 0$ of the Hamiltonian flow

$$\partial_s \begin{pmatrix} \eta \\ \zeta \end{pmatrix} = \begin{pmatrix} 0 & 1 \\ -1 & 0 \end{pmatrix} \begin{pmatrix} \partial_\eta K^{(3)} \\ \partial_\zeta K^{(3)} \end{pmatrix}, \tag{3.28}$$

with initial conditions at $s = -1$ being the original variables.

To write $K^{(3)}$ in the physical space, it is convenient to introduce $\tilde{\eta} = \mathrm{H}\eta$, $\tilde{\zeta} = \mathrm{H}\zeta$, where $\mathrm{H} = -\mathrm{i}\,\mathrm{sgn}(D)$ is the Hilbert transform. In the following, we will use the identities $\mathrm{H}\,|D| = -\partial_x$, $\mathrm{H}\,|D|^{-1} = \partial_x^{-1}$, and similar ones.

PROPOSITION 3.2. *The auxiliary Hamiltonian $K^{(3)}$ in* (3.20) *can be written in the physical space as*

$$\begin{aligned}
K^{(3)} = \int \Bigg[&\frac{1}{2}\,\tilde{\eta}^2\,\partial_x\tilde{\zeta} - \frac{\gamma}{4g}\,(g\eta^2\tilde{\eta} - \zeta^2\,\partial_x\eta + 2\zeta\tilde{\eta}\,\partial_x\tilde{\zeta}) \\
&- \frac{\gamma^2}{4g^2}\left(g(\partial_x^{-1}\eta)(\partial_x\eta)\zeta + g\eta\tilde{\eta}\tilde{\zeta} - g\tilde{\eta}(\partial_x\tilde{\zeta})\,\partial_x^{-1}\eta - \frac{1}{2}\,\zeta^2\,\partial_x\tilde{\zeta}\right) \\
&- \frac{\gamma^3}{16g^2}\left(\zeta^2\tilde{\eta} + 2\zeta(\partial_x\tilde{\zeta})\partial_x^{-1}\,\eta - 2g(\partial_x^{-1}\eta)(\partial_x\tilde{\eta})(\partial_x^{-1}\tilde{\eta})\right) \\
&- \frac{\gamma^4}{16g^2}\,(\eta\tilde{\zeta} - \tilde{\eta}\zeta)\,\partial_x^{-1}\eta - \frac{\gamma^5}{64g^2}\,\tilde{\eta}(\partial_x^{-1}\eta)^2\Bigg]\,\mathrm{d}x. \tag{3.29}
\end{aligned}$$

Proof. The main idea is to expand the brackets in the expression (3.20) for $K^{(3)}$, identify terms and combine them appropriately. We decompose $K^{(3)}$ as

$$K^{(3)} = \mathrm{I} + \mathrm{II} + \mathrm{III} + \mathrm{IV}, \tag{3.30}$$

where I is the part of $K^{(3)}$ associated with $\eta\eta\eta$-type terms, namely

$$\begin{aligned}
\mathrm{I} = \frac{1}{4\mathrm{i}\sqrt{2\pi}}\int (1 + \mathrm{sgn}(k_1)\,\mathrm{sgn}(k_3))\left(\frac{\dfrac{\gamma^4}{8} + \dfrac{\gamma^2}{2}\,g\,|k_2| + g^2\,|k_1|\,|k_3|}{g^2\,|k_1|\,|k_3|}\right)\frac{\gamma}{2} \\
\times \mathrm{sgn}(k_2)\,\eta_1\eta_2\eta_3\,\delta_{123}\,\mathrm{d}k_{123}. \tag{3.31}
\end{aligned}$$

The part II is associated with $\eta\eta\zeta$-type terms, III is associated with $\eta\zeta\zeta$-type terms, and IV is associated with $\zeta\zeta\zeta$-type terms. Below, we give the computations for I. The remaining terms can be computed in a similar way. We further decompose I into a sum of three terms $\mathrm{I} = \mathrm{I}_1 + \mathrm{I}_2 + \mathrm{I}_3$ based on the power of γ involved:

$$\left.\begin{aligned}
\mathrm{I}_1 &= \frac{\gamma^5}{64\mathrm{i}g^2\sqrt{2\pi}}\int (1 + \mathrm{sgn}(k_1)\,\mathrm{sgn}(k_3))\,\frac{1}{|k_1|\,|k_3|}\,\mathrm{sgn}(k_2)\,\eta_1\eta_2\eta_3\,\delta_{123}\,\mathrm{d}k_{123}, \\
\mathrm{I}_2 &= \frac{\gamma^3}{16\mathrm{i}g\sqrt{2\pi}}\int (1 + \mathrm{sgn}(k_1)\,\mathrm{sgn}(k_3))\,\frac{|k_2|}{|k_1|\,|k_3|}\,\mathrm{sgn}(k_2)\,\eta_1\eta_2\eta_3\,\delta_{123}\,\mathrm{d}k_{123}, \\
\mathrm{I}_3 &= \frac{\gamma}{8\mathrm{i}\sqrt{2\pi}}\int (1 + \mathrm{sgn}(k_1)\,\mathrm{sgn}(k_3))\,\mathrm{sgn}(k_2)\,\eta_1\eta_2\eta_3\,\delta_{123}\,\mathrm{d}k_{123}.
\end{aligned}\right\} \tag{3.32}$$

Writing $\mathrm{sgn}(k_2) = k_2/|k_2|$ in I_1, we get

$$
\mathrm{I}_1 = \frac{\gamma^5}{64 \mathrm{i} g^2 \sqrt{2\pi}} \int \frac{k_2}{|k_1| \, |k_2| \, |k_3|} \, \eta_1 \eta_2 \eta_3 \, \delta_{123} \, \mathrm{d}k_{123}
$$
$$
+ \frac{\gamma^5}{64 \mathrm{i} g^2 \sqrt{2\pi}} \int \frac{\mathrm{sgn}(k_1) \, \mathrm{sgn}(k_2) \, \mathrm{sgn}(k_3)}{|k_1| \, |k_3|} \, \eta_1 \eta_2 \eta_3 \, \delta_{123} \, \mathrm{d}k_{123} = \mathrm{I}_1^{(1)} + \mathrm{I}_1^{(2)}. \quad (3.33)
$$

Using the index rearrangements $(k_1, k_2, k_3) \to (k_2, k_1, k_3)$ and $(k_1, k_2, k_3) \to (k_1, k_3, k_2)$, we see that $\mathrm{I}_1^{(1)} = 0$ since the integration is over $k_1 + k_2 + k_3 = 0$. The part I_1 thus reduces to

$$
\mathrm{I}_1 = \frac{\gamma^5}{64 \mathrm{i} g^2 \sqrt{2\pi}} \int \frac{\mathrm{sgn}(k_2)}{k_1 k_3} \, \eta_1 \eta_2 \eta_3 \, \delta_{123} \, \mathrm{d}k_{123} = -\frac{\gamma^5}{64 g^2} \int (\partial_x^{-1} \eta)^2 \tilde{\eta} \, \mathrm{d}x. \quad (3.34)
$$

Similar steps imply

$$
\mathrm{I}_2 = \frac{\gamma^3}{8g} \int (\partial_x^{-1} \eta)(\partial_x \tilde{\eta})(\partial_x^{-1} \eta) \, \mathrm{d}x, \quad \mathrm{I}_3 = -\frac{\gamma}{4} \int \eta^2 \tilde{\eta} \, \mathrm{d}x. \quad (3.35a,b)
$$

Combining (3.34)–(3.35a,b),

$$
\mathrm{I} = -\frac{\gamma}{4} \int \eta^2 \tilde{\eta} \, \mathrm{d}x + \frac{\gamma^3}{8g} \int (\partial_x^{-1} \eta)(\partial_x \tilde{\eta})(\partial_x^{-1} \tilde{\eta}) \, \mathrm{d}x - \frac{\gamma^5}{64 g^2} \int (\partial_x^{-1} \eta)^2 \tilde{\eta} \, \mathrm{d}x, \quad (3.36)
$$

which are the second, eleventh and fourteenth terms in (3.29). Terms II, III and IV are calculated in a similar fashion and identify to the remaining terms in (3.29). ∎

We now apply the variational derivatives ∂_η and ∂_ζ on $K^{(3)}$ to obtain the third-order normal form transformation defining the Hamiltonian flow (3.28).

PROPOSITION 3.3. *The Hamiltonian system that defines the third-order normal form transformation has the form of a system of two partial differential equations:*

$$
\partial_s \eta = \partial_\zeta K^{(3)} = \frac{1}{2} \mathrm{H} \, \partial_x \tilde{\eta}^2 + \frac{\gamma}{2g} \left(\zeta \, \partial_x \eta - \tilde{\eta} \, \partial_x \tilde{\zeta} - |D| \, (\zeta \tilde{\eta}) \right)
$$
$$
+ \frac{\gamma^2}{4g^2} \left(\zeta \, \partial_x \tilde{\zeta} + \frac{1}{2} |D| \, \zeta^2 \right) + \frac{\gamma^2}{4g} \left(-(\partial_x^{-1} \eta)(\partial_x \eta) + \mathrm{H}(\eta \tilde{\eta}) + |D| \, (\tilde{\eta} \, \partial_x^{-1} \eta) \right)
$$
$$
- \frac{\gamma^3}{8g^2} \left(\zeta \tilde{\eta} + (\partial_x \tilde{\zeta})(\partial_x^{-1} \eta) + |D| \, (\zeta \, \partial_x^{-1} \eta) \right) + \frac{\gamma^4}{16 g^2} \left(\mathrm{H}(\eta \, \partial_x^{-1} \eta) + \tilde{\eta} \, \partial_x^{-1} \eta \right),
$$
$$
(3.37)
$$

$$\partial_s \zeta = -\partial_\eta K^{(3)} = \mathrm{H}(\tilde{\eta}\, \partial_x \tilde{\zeta}) + \frac{\gamma}{2} \left(\eta \tilde{\eta} - \frac{1}{2} \mathrm{H}(\eta^2) \right) + \frac{\gamma}{2g} \left(\zeta\, \partial_x \zeta - \mathrm{H}(\zeta\, \partial_x \tilde{\zeta}) \right)$$

$$- \frac{\gamma^2}{4g} \left(\partial_x(\zeta\, \partial_x^{-1}\eta) + \partial_x^{-1}(\zeta\, \partial_x \eta) - \tilde{\zeta}\tilde{\eta} + \mathrm{H}(\eta\tilde{\zeta}) \right.$$

$$\left. -\mathrm{H}\left((\partial_x \tilde{\zeta})(\partial_x^{-1}\eta) \right) - \partial_x^{-1}\left((\partial_x \tilde{\zeta})\tilde{\eta} \right) \right)$$

$$+ \frac{\gamma^3}{8g} \left(\partial_x^{-1}\left((\partial_x \tilde{\eta})(\partial_x^{-1}\tilde{\eta}) \right) - |D|\left((\partial_x^{-1}\eta)(\partial_x^{-1}\tilde{\eta}) \right) + |D|^{-1}\left((\partial_x \tilde{\eta})(\partial_x^{-1}\eta) \right) \right)$$

$$- \frac{\gamma^3}{16g^2} \left(\mathrm{H}(\zeta^2) + 2\, \partial_x^{-1}(\zeta\, \partial_x \tilde{\zeta}) \right)$$

$$+ \frac{\gamma^4}{16g^2} \left(\tilde{\zeta}\, \partial_x^{-1}\eta - \partial_x^{-1}(\eta\tilde{\zeta}) + \mathrm{H}(\zeta\, \partial_x^{-1}\eta) + \partial_x^{-1}(\zeta\tilde{\eta}) \right)$$

$$- \frac{\gamma^5}{64g^2} \left(\mathrm{H}\left((\partial_x^{-1}\eta)^2 \right) + 2\, \partial_x^{-1}\left(\tilde{\eta}\, \partial_x^{-1}\eta \right) \right). \tag{3.38}$$

In the absence of vorticity ($\gamma = 0$), the equation for η simplifies to $\partial_s \eta = \frac{1}{2}\mathrm{H}\, \partial_x(\tilde{\eta})^2$, or equivalently, to the inviscid Burgers equation for $\tilde{\eta}$,

$$\partial_s \tilde{\eta} + \tilde{\eta}\, \partial_x \tilde{\eta} = 0, \tag{3.39}$$

as obtained by Craig & Sulem (2016), while $\tilde{\zeta}$ satisfies

$$\partial_s \tilde{\zeta} + \tilde{\eta}\, \partial_x \tilde{\zeta} = 0, \tag{3.40}$$

which is its linearization along the Burgers flow. These equations were tested in Craig *et al.* (2021*a*) and Guyenne *et al.* (2021, 2022) in the context of irrotational gravity waves on deep water.

Due to the complexity of the formulas for $\partial_\eta K^{(3)}$ and $\partial_\zeta K^{(3)}$, we have checked *a posteriori* that the cohomology equation (3.17) is indeed satisfied.

4. Reduced Hamiltonian

In this section, we analyse the new Hamiltonian $\mathcal{H}'$ obtained after applying the third-order normal form transformation given by the flow of the auxiliary Hamiltonian system (3.28). By construction, such a transformation removes all cubic homogeneous terms based on (3.17). For simplicity, we now drop the primes from all new quantities. From (3.16), the new Hamiltonian becomes

$$\mathcal{H}(w) = \mathcal{H}^{(2)}(w) + \mathcal{H}^{(4)}(w) - \{K^{(3)}, \mathcal{H}^{(3)}\}(w) + \frac{1}{2}\{K^{(3)}, \{K^{(3)}, \mathcal{H}^{(2)}\}\}(w) + R^{(5)}$$

$$= \mathcal{H}^{(2)}(w) + \mathcal{H}_+^{(4)}(w) + R^{(5)}, \tag{4.1}$$

where $R^{(5)}$ denotes all terms of order 5 and higher, and $\mathcal{H}_+^{(4)}$ is the new fourth-order term

$$\mathcal{H}_+^{(4)} = \mathcal{H}^{(4)} - \frac{1}{2}\{K^{(3)}, \mathcal{H}^{(3)}\}. \tag{4.2}$$

Our approximation is based on the quadratic and quartic homogeneous terms of $\mathcal{H}$. The quadratic term is given by (2.36) in terms of new complex symplectic coordinates. The

949 A50-16

quartic term $\mathcal{H}^{(4)}_+$ is more complicated and requires careful computations. Since the latter is homogeneous of degree 4 in η and ζ, every monomial appearing in $\mathcal{H}^{(4)}_+$ is of type $A_1 A_2 A_3 A_4$, with A_j being η or ζ. Equivalently, in terms of the complex symplectic coordinates (2.33), it has the form of a sum of integrals with all possible combinations of fourth-order monomials in z_k and $\bar{z}_{-k}$:

$$\mathcal{H}^{(4)}_+ = \int \left[T^+ z_1 z_2 z_3 z_4 + T^\pm z_1 z_2 z_3 \bar{z}_{-4} + T^+_- z_1 z_2 \bar{z}_{-3} \bar{z}_{-4} + T^\mp z_1 \bar{z}_{-2} \bar{z}_{-3} \bar{z}_{-4} \right. \tag{4.3}$$
$$\left. + T^- \bar{z}_{-1} \bar{z}_{-2} \bar{z}_{-3} \bar{z}_{-4} \right] \delta_{1234} \, \mathrm{d}k_{1234},$$

where T^+, $T^\pm$, T^+_-, $T^\mp$ and T^- are coefficients depending on k_1, k_2, k_3 and k_4. In view of the subsequent modulational ansatz and homogenization process, it is not necessary to calculate explicitly all the coefficients above. As shown in Guyenne *et al.* (2022), under the modulational ansatz, only the third term in (4.3) is relevant as the other terms are negligible due to scale separation. Therefore, we will calculate only the term

$$\mathcal{H}^{(4)}_{+R} = \int T^+_- z_1 z_2 \bar{z}_{-3} \bar{z}_{-4} \, \delta_{1234} \, \mathrm{d}k_{1234}, \tag{4.4}$$

which is, after index rearrangement $(k_1, k_2, k_3, k_4) \rightarrow (k_1, k_2, -k_3, -k_4)$,

$$\mathcal{H}^{(4)}_{+R} = \int T z_1 z_2 \bar{z}_3 \bar{z}_4 \, \delta_{1+2-3-4} \, \mathrm{d}k_{1234}. \tag{4.5}$$

Denoting

$$\mathcal{H}^{(4)}_R = \int T_1 z_1 z_2 \bar{z}_3 \bar{z}_4 \, \delta_{1+2-3-4} \, \mathrm{d}k_{1234}, \quad \{K^{(3)}, \mathcal{H}^{(3)}\}_R = \int T_2 z_1 z_2 \bar{z}_3 \bar{z}_4 \, \delta_{1+2-3-4} \, \mathrm{d}k_{1234}, \tag{4.6a,b}$$

the contributions from $zz\bar{z}\bar{z}$-type monomials to $\mathcal{H}^{(4)}$ and $\{K^{(3)}, \mathcal{H}^{(3)}\}$, respectively, we have

$$T = T_1 - \tfrac{1}{2} T_2. \tag{4.7}$$

The precise formulas for the coefficients T_1 and T_2 are given in the next two propositions.

PROPOSITION 4.1. *We have* $T_1 = T^{(1)}_1 + T^{(2)}_1 + T^{(3)}_1$, *where*

$$\left.\begin{aligned}
T^{(1)}_1 &= -D^{(1)}_{12(-3)(-4)} - D^{(1)}_{(-4)(-3)21} - D^{(1)}_{1(-3)2(-4)} - D^{(1)}_{(-4)2(-3)1} + D^{(1)}_{1(-4)(-3)2} + D^{(1)}_{(-4)21(-3)}, \\
T^{(2)}_1 &= D^{(2)}_{12(-3)(-4)} - D^{(2)}_{(-4)(-3)21} + D^{(2)}_{1(-3)2(-4)} - D^{(2)}_{(-4)2(-3)1} + D^{(2)}_{1(-4)(-3)2} - D^{(2)}_{(-4)21(-3)}, \\
T^{(3)}_1 &= D^{(3)}_{12(-3)(-4)} + D^{(3)}_{(-4)(-3)21} + D^{(3)}_{1(-3)2(-4)} + D^{(3)}_{(-4)2(-3)1} + D^{(3)}_{1(-4)(-3)2} + D^{(3)}_{(-4)21(-3)},
\end{aligned}\right\} \tag{4.8}$$

with

$$\left.\begin{aligned}
D^{(1)}_{1234} &= \frac{a_1 a_4}{32\pi a_2 a_3} |k_1| \, |k_4| \, (|k_1| + |k_4| - 2|k_3 + k_4|), \\
D^{(2)}_{1234} &= \frac{\gamma a_1}{32\pi a_2 a_3 a_4} |k_1| \, \mathrm{sgn}(k_4) \, (|k_1| + |k_4| - |k_3 + k_4| - |k_3 + k_1|), \\
D^{(3)}_{1234} &= \frac{\gamma^2}{128\pi a_1 a_2 a_3 a_4} \mathrm{sgn}(k_1) \, \mathrm{sgn}(k_4) \, (|k_1| + |k_4| - 2|k_3 + k_4|).
\end{aligned}\right\} \tag{4.9}$$

Proof. Expanding the brackets in the expression (2.29) of $\mathcal{H}^{(4)}$, we have

$$
\mathcal{H}^{(4)} = -\frac{1}{8\pi} \int |k_1| \, |k_4| \, (|k_1| + |k_4| - 2|k_3 + k_4|)
$$
$$
\times \left(\zeta_1 \eta_2 \eta_3 \zeta_4 - \frac{i\gamma}{2k_1} \eta_1 \eta_2 \eta_3 \zeta_4 - \frac{i\gamma}{2k_4} \zeta_1 \eta_2 \eta_3 \eta_4 - \frac{\gamma^2}{4k_1 k_4} \eta_1 \eta_2 \eta_3 \eta_4 \right) \delta_{1234} \, \mathrm{d}k_{1234}.
$$
(4.10)

The terms associated with $\eta_1 \eta_2 \eta_3 \zeta_4$ and $\zeta_1 \eta_2 \eta_3 \eta_4$ can be combined by using the index rearrangement $(k_1, k_2, k_3, k_4) \rightarrow (k_4, k_2, k_3, k_1)$, and we obtain

$$
\mathcal{H}^{(4)} = -\frac{1}{8\pi} \int |k_1| \, |k_4| \, (|k_1| + |k_4| - 2|k_3 + k_4|) \zeta_1 \eta_2 \eta_3 \zeta_4 \, \delta_{1234} \, \mathrm{d}k_{1234}
$$
$$
+ \frac{1}{8\pi} \int |k_1| \, |k_4| \, (|k_1| + |k_4| - |k_3 + k_4| - |k_3 + k_1|) \frac{i\gamma}{k_4} \zeta_1 \eta_2 \eta_3 \eta_4 \, \delta_{1234} \, \mathrm{d}k_{1234}
$$
$$
+ \frac{1}{8\pi} \int |k_1| \, |k_4| \, (|k_1| + |k_4| - 2|k_3 + k_4|) \frac{\gamma^2}{4k_1 k_4} \eta_1 \eta_2 \eta_3 \eta_4 \, \delta_{1234} \, \mathrm{d}k_{1234}
$$
$$
:= \mathrm{I} + \mathrm{II} + \mathrm{III}.
$$
(4.11)

We then write (η, ζ) in terms of $(z, \bar{z})$, and retain only monomials of type $zz\bar{z}\bar{z}$. Denoting I_R, II_R, III_R the corresponding terms in (4.11), we find

$$
\mathrm{I}_R = \int D^{(1)}_{1234} (-z_1 z_2 \bar{z}_{-3} \bar{z}_{-4} - z_1 \bar{z}_{-2} z_3 \bar{z}_{-4} + z_1 \bar{z}_{-2} \bar{z}_{-3} z_4
$$
$$
+ \bar{z}_{-1} z_2 z_3 \bar{z}_{-4} - \bar{z}_{-1} z_2 \bar{z}_{-3} z_4 - \bar{z}_{-1} \bar{z}_{-2} z_3 z_4) \, \delta_{1234} \, \mathrm{d}k_{1234}.
$$
(4.12)

We turn all monomials in the above expression into $z_1 z_2 \bar{z}_3 \bar{z}_4$ by transforming indices in an appropriate way, leading to

$$
\mathrm{I}_R = \int T^{(1)}_1 z_1 z_2 \bar{z}_3 \bar{z}_4 \, \delta_{1+2-3-4} \, \mathrm{d}k_{1234},
$$
(4.13)

as well as

$$
\mathrm{II}_R = \int T^{(2)}_1 z_1 z_2 \bar{z}_3 \bar{z}_4 \, \delta_{1+2-3-4} \, \mathrm{d}k_{1234}, \quad \mathrm{III}_R = \int T^{(3)}_1 z_1 z_2 \bar{z}_3 \bar{z}_4 \, \delta_{1+2-3-4} \, \mathrm{d}k_{1234}.
$$
(4.14a,b)

∎

To find the explicit expression for the coefficient T_2 of $\{K^{(3)}, \mathcal{H}^{(3)}\}_R$, we follow the steps in Appendix B of our recent paper (Guyenne *et al.* 2022). The main idea is to use (3.22) to expand the Poisson bracket $\{K^{(3)}, \mathcal{H}^{(3)}\}$ according to (2.40), and extract terms of $zz\bar{z}\bar{z}$-type.

PROPOSITION 4.2. *We have* $T_2 = T_2^{(1)} + T_2^{(2)} + T_2^{(3)}$, *with*

$$T_2^{(1)} = \frac{1}{64\pi} \left(S_{(-1-2)12} + S_{2(-1-2)1} + S_{12(-1-2)} \right) \left(S_{(-3-4)34} + S_{4(-3-4)3} + S_{34(-3-4)} \right)$$

$$\times \left(\frac{1}{\Omega_1 + \Omega_2 + \Omega_{-1-2}} + \frac{1}{\Omega_3 + \Omega_4 + \Omega_{-3-4}} \right), \tag{4.15}$$

$$T_2^{(2)} = -A_{(-1)(-2)(1+2)} A_{(-3)(-4)(3+4)} \left(\frac{1}{\Omega_1 + \Omega_2 - \Omega_{1+2}} + \frac{1}{\Omega_3 + \Omega_4 - \Omega_{3+4}} \right), \tag{4.16}$$

$$T_2^{(3)} = 4 A_{(1-3)(-1)3} A_{(4-2)(-4)2} \left(\frac{1}{\Omega_{3-1} + \Omega_1 - \Omega_3} + \frac{1}{\Omega_{2-4} + \Omega_4 - \Omega_2} \right). \tag{4.17}$$

Proof. The Poisson bracket of the cubic Hamiltonian (3.22) contains $zz\bar{z}\bar{z}$-type terms given by

$$i\{K^{(3)}, \mathcal{H}^{(3)}\}_R = \left\{ \int \frac{A_{123} z_1 z_2 z_3}{\Omega_1 + \Omega_2 + \Omega_3} \delta_{123} \, dk_{123}, \int A_{456} \bar{z}_4 \bar{z}_5 \bar{z}_6 \delta_{456} \, dk_{456} \right\}$$

$$- \left\{ \int \frac{A_{123} \bar{z}_1 \bar{z}_2 \bar{z}_3}{\Omega_1 + \Omega_2 + \Omega_3} \delta_{123} \, dk_{123}, \int A_{456} z_4 z_5 z_6 \delta_{456} \, dk_{456} \right\}$$

$$+ \left\{ \int \frac{A_{123} z_{-1} z_{-2} \bar{z}_3}{\Omega_{-1} + \Omega_{-2} - \Omega_3} \delta_{123} \, dk_{123}, \int A_{456} \bar{z}_{-4} \bar{z}_{-5} z_6 \delta_{456} \, dk_{456} \right\}$$

$$- \left\{ \int \frac{A_{123} \bar{z}_{-1} \bar{z}_{-2} z_3}{\Omega_{-1} + \Omega_{-2} - \Omega_3} \delta_{123} \, dk_{123}, \int A_{456} z_{-4} z_{-5} \bar{z}_6 \delta_{456} \, dk_{456} \right\}$$

$$:= i(R_1 + R_2 + R_3 + R_4), \tag{4.18}$$

where we denote each line of (4.18) by R_1, R_2, R_3, R_4, respectively. We obtain

$$\left. \begin{aligned} R_1 + R_2 &= \int T_2^{(1)} z_1 z_2 \bar{z}_3 \bar{z}_4 \, \delta_{1+2-3-4} \, dk_{1234}, \\ R_3 + R_4 &= \int (T_2^{(2)} + T_2^{(3)}) z_1 z_2 \bar{z}_3 \bar{z}_4 \, \delta_{1+2-3-4} \, dk_{1234}. \end{aligned} \right\} \tag{4.19}$$

We refer to Guyenne *et al.* (2022) for more details on such computations. ∎

5. Modulational ansatz

We restrict our interest to solutions in the form of near-monochromatic waves with carrier wavenumber $k_0 > 0$. In the Fourier space, this corresponds to a narrowband approximation with η_k and ζ_k localized near k_0. Equivalently, z_k and $\bar{z}_k$ are also localized around k_0. As it was pointed out earlier, such assumptions allow us to simplify the analysis of the quartic part $\mathcal{H}_+^{(4)}$ in (4.3), as several of its terms become negligible. This is indeed a problem of homogenization, which is treated via a scale separation lemma (see Lemma 4.4 of Guyenne *et al.* 2022). This homogenization naturally selects the term (4.5) in $\mathcal{H}_+^{(4)}$, namely the four-wave resonances, among all the possible quartic interactions as this term involves fast oscillations that cancel out exactly. Its coefficient T can be found according to (4.7).

The full expression of this coefficient is given by the combination of results in Propositions 4.1 and 4.2. These expressions, however, simplify in the modulational regime.

We introduce the modulational ansatz

$$k = k_0 + \varepsilon\lambda, \quad \text{where } \frac{\lambda}{k_0} = O(1), \ \varepsilon \ll 1, \tag{5.1}$$

which captures the slow modulation of small-amplitude near-monochromatic waves with carrier wavenumber $k_0 > 0$. The small dimensionless parameter ε is a measure of the wave spectrum's narrowness around $k = k_0$. Accordingly, we define the function U as

$$U(\lambda) = z(k_0 + \varepsilon\lambda), \quad \bar{U}(\lambda) = \bar{z}(k_0 + \varepsilon\lambda), \tag{5.2a,b}$$

in the Fourier space, where the time dependence is omitted. In the physical space,

$$z(x) = \frac{1}{\sqrt{2\pi}} \int z(k)\, e^{ikx}\, dk = \frac{\varepsilon}{\sqrt{2\pi}} \int U(\lambda)\, e^{ik_0x}\, e^{i\lambda\varepsilon x}\, d\lambda = \varepsilon\, u(X)\, e^{ik_0x}, \tag{5.3}$$

where u, as a function of the long spatial scale $X = \varepsilon x$, is the inverse Fourier transform of U. Equation (5.3) indicates that the dimensionless parameter ε may also be related to some measure of the wave steepness.

To calculate the quartic interactions in the modulational regime, we approximate the coefficients in Propositions 4.1 and 4.2 under the modulational ansatz (5.1). First, we need a few simple expansions that are summarized in the lemma below.

LEMMA 5.1. *Under the modulational ansatz* (5.1)*, we have the following expansions:*

$$\left.\begin{array}{c} |k| = k_0 + \varepsilon\lambda + O(\varepsilon^4), \quad \mathrm{sgn}(k) = 1 + O(\varepsilon^5), \quad \omega_k = \omega_0\left(1 + \varepsilon\frac{g}{2\omega_0^2}\lambda\right) + O(\varepsilon^2), \\[3mm] a_k = \sqrt{\frac{\omega_0}{k_0}}\left(1 + \frac{\varepsilon}{4}\left(\frac{g}{\omega_0^2} - \frac{2}{k_0}\right)\lambda\right) + O(\varepsilon^2), \\[3mm] a_{1-3} = a(k_1 - k_3) = \frac{\sqrt{|\gamma|}}{\sqrt{2}\,\varepsilon^{1/2}\,|\lambda_1 - \lambda_3|^{1/2}}\left(1 + \frac{\varepsilon g}{\gamma^2}|\lambda_1 - \lambda_3|\right) + O(\varepsilon^{3/2}), \\[3mm] \omega_{1-3} = \frac{|\gamma|}{2}\left(1 + \frac{2g\varepsilon}{\gamma^2}|\lambda_1 - \lambda_3|\right) + O(\varepsilon^2). \end{array}\right\} \tag{5.4}$$

LEMMA 5.2. *Under the modulational ansatz* (5.1)*, we have*

$$\int T_1 z_1 z_2 \bar{z}_3 \bar{z}_4\, \delta_{1+2-3-4}\, dk_{1234} = \varepsilon^3 \int \left(c_0^l + \varepsilon c_0^r(\lambda_2 + \lambda_3)\right) U_1 U_2 \bar{U}_3 \bar{U}_4\, \delta_{1+2-3-4}\, d\lambda_{1234}$$
$$+ O(\varepsilon^5), \tag{5.5}$$

where $U_j := U(\lambda_j)$, T_1 is given in Proposition 4.1, and the coefficients are

$$c_0^l = \frac{k_0^3 \Omega_0^2}{8\pi\omega_0^2}, \quad c_0^r = \frac{3k_0^2\Omega_0^2}{16\pi\omega_0^2} - \frac{\gamma g k_0^3 \Omega_0}{32\pi\omega_0^4}. \tag{5.6a,b}$$

Proof. As given in Proposition 4.1, T_1 is the sum of several terms, all involving coefficients similar to $D_{1234}^{(1)}$. The latter includes only factors of type $|k_j|$ and a_j, and expansion of these factors is given in the lemma above. For $D_{12(-3)(-4)}^{(1)}$, we write

$$D_{12(-3)(-4)}^{(1)} = -\frac{k_0^3}{16\pi} \left(1 + \frac{\varepsilon}{2k_0} (\lambda_2 + 3\lambda_3 + 2\lambda_4) + \frac{\varepsilon g}{4\omega_0^2} (\lambda_1 - \lambda_2 - \lambda_3 + \lambda_4) \right) + O(\varepsilon^2).$$

(5.7)

The brackets above simplify in the integration due to the symmetry of $z_1 z_2 \bar{z}_3 \bar{z}_4$ under index rearrangements and the presence of the delta function $\delta_{1+2-3-4}$, yielding

$$\int -D_{12(-3)(-4)}^{(1)} z_1 z_2 \bar{z}_3 \bar{z}_4 \, \delta_{1+2-3-4} \, \mathrm{d}k_{1234}$$
$$= \int \left(\frac{k_0^3}{16\pi} + \frac{3\varepsilon k_0^2}{32\pi} (\lambda_2 + \lambda_3) \right) z_1 z_2 \bar{z}_3 \bar{z}_4 \, \delta_{1+2-3-4} \, \mathrm{d}k_{1234}.$$

(5.8)

The remaining computations are similar, and we have

$$\int T_1^{(1)} z_1 z_2 \bar{z}_3 \bar{z}_4 \, \delta_{1+2-3-4} \, \mathrm{d}k_{1234} = \int \left(\frac{k_0^3}{8\pi} + \frac{3\varepsilon k_0^2}{16\pi} (\lambda_2 + \lambda_3) \right) z_1 z_2 \bar{z}_3 \bar{z}_4 \, \delta_{1+2-3-4} \, \mathrm{d}k_{1234},$$

(5.9)

$$\int T_1^{(2)} z_1 z_2 \bar{z}_3 \bar{z}_4 \, \delta_{1+2-3-4} \, \mathrm{d}k_{1234} = \int \left(\frac{\gamma k_0^3}{8\pi\omega_0} + \frac{\varepsilon\gamma k_0^3}{8\pi\omega_0} \left(\frac{3}{2k_0} - \frac{g}{4\omega_0^2} \right) (\lambda_2 + \lambda_3) \right)$$
$$\times z_1 z_2 \bar{z}_3 \bar{z}_4 \, \delta_{1+2-3-4} \, \mathrm{d}k_{1234},$$

(5.10)

$$\int T_1^{(3)} z_1 z_2 \bar{z}_3 \bar{z}_4 \, \delta_{1+2-3-4} \, \mathrm{d}k_{1234} = \int \left(\frac{\gamma^2 k_0^3}{32\pi\omega_0^2} + \frac{\varepsilon\gamma^2 k_0^3}{32\pi\omega_0^2} \left(\frac{3}{2k_0} - \frac{g}{2\omega_0^2} \right) (\lambda_2 + \lambda_3) \right)$$
$$\times z_1 z_2 \bar{z}_3 \bar{z}_4 \, \delta_{1+2-3-4} \, \mathrm{d}k_{1234}.$$

(5.11)

Using that $T_1 = T_1^{(1)} + T_1^{(2)} + T_1^{(3)}$, we get

$$\int T_1 z_1 z_2 \bar{z}_3 \bar{z}_4 \, \delta_{1+2-3-4} \, \mathrm{d}k_{1234} = \int \left(c_0^l + \varepsilon c_0^r (\lambda_2 + \lambda_3) \right) z_1 z_2 \bar{z}_3 \bar{z}_4 \, \delta_{1+2-3-4} \, \mathrm{d}k_{1234}$$
$$+ O(\varepsilon^2).$$

(5.12)

Writing the right-hand side in terms of U given by (5.2*a,b*), and using that $\delta(k_1 + k_2 - k_3 - k_4) = \varepsilon^{-1}\delta(\lambda_1 + \lambda_2 - \lambda_3 - \lambda_4)$, we obtain the desired result. ∎

LEMMA 5.3. *Under the modulational ansatz* (5.1), *we have*

$$\int T_2^{(1)} z_1 z_2 \bar{z}_3 \bar{z}_4 \, \delta_{1+2-3-4} \, dk_{1234} = \varepsilon^3 \int \left(c_1^l + \varepsilon c_1^r (\lambda_2 + \lambda_3) \right) U_1 U_2 \bar{U}_3 \bar{U}_4 \, \delta_{1+2-3-4} \, d\lambda_{1234}$$
$$+ O(\varepsilon^5), \tag{5.13}$$

$$\int T_2^{(2)} z_1 z_2 \bar{z}_3 \bar{z}_4 \, \delta_{1+2-3-4} \, dk_{1234} = \varepsilon^3 \int \left(c_2^l + \varepsilon c_2^r (\lambda_2 + \lambda_3) \right) U_1 U_2 \overline{U}_3 \overline{U}_4 \, \delta_{1+2-3-4} \, d\lambda_{1234}$$
$$+ O(\varepsilon^5), \tag{5.14}$$

$$\int T_2^{(3)} z_1 z_2 \bar{z}_3 \bar{z}_4 \, \delta_{1+2-3-4} \, dk_{1234} = \varepsilon^3 \int \left(c_3^l + \varepsilon c_3^{r,1} (\lambda_2 + \lambda_3) + \varepsilon c_3^{r,2} |\lambda_1 - \lambda_3| \right)$$
$$\times \, U_1 U_2 \bar{U}_3 \bar{U}_4 \, \delta_{1+2-3-4} \, d\lambda_{1234} + O(\varepsilon^5), \tag{5.15}$$

where

$$\left. \begin{aligned}
c_1^l &= \frac{k_0^3 (2\omega_0^2 + \gamma \omega_{2k_0})^2}{16\pi \omega_0^2 \omega_{2k_0} (2\Omega_0 + \Omega_{-2k_0})}, \quad \Omega_{\pm 2k_0} = \frac{\gamma}{2} \operatorname{sgn}(\pm 2k_0) + \omega_{2k_0}, \\
c_1^r &= g c_1^l \left(\frac{2\Omega_{2k_0}}{\omega_{2k_0} (2\omega_0^2 + \gamma \omega_{2k_0})} - \frac{1}{2\omega_0^2} - \frac{1}{2\omega_{2k_0}^2} + \frac{3}{2g k_0} - \frac{\omega_{2k_0} + \omega_0}{2\omega_{2k_0} \omega_0 (2\Omega_0 + \Omega_{-2k_0})} \right), \\
c_2^l &= -\frac{k_0^3 (2\omega_0^2 - \gamma \omega_{2k_0})^2}{16\pi \omega_0^2 \omega_{2k_0} (2\Omega_0 - \Omega_{2k_0})}, \\
c_2^r &= g c_2^l \left(\frac{2\Omega_{-2k_0}}{\omega_{2k_0} (2\omega_0^2 - \gamma \omega_{2k_0})} - \frac{1}{2\omega_0^2} - \frac{1}{2\omega_{2k_0}^2} + \frac{3}{2g k_0} - \frac{\omega_{2k_0} - \omega_0}{2\omega_{2k_0} \omega_0 (2\Omega_0 - \Omega_{2k_0})} \right), \\
c_3^l &= \frac{\gamma^2 k_0^2 \omega_0}{2\pi g \Omega_0}, \quad c_3^{r,1} = c_3^l \left(\frac{1}{k_0} + \frac{g\gamma}{8\Omega_0 \omega_0^2} \right), \quad c_3^{r,2} = \frac{k_0^2 \omega_0^2}{2\pi \Omega_0^2}.
\end{aligned} \right\} \tag{5.16}$$

Proof. The proof is given in Appendix A. ∎

The leading coefficients in the expansions of Lemmas 5.2 and 5.3 combine together as

$$c_0^l - \frac{1}{2} \left(c_1^l + c_2^l + c_3^l \right) = \frac{k_0^3 (\omega_0 - \gamma)(\gamma^2 + 4\omega_0^2)}{8\pi \omega_0 \Omega_0 (2\omega_0 - \gamma)}. \tag{5.17}$$

Denoting

$$\beta := 8\pi \left[c_0^r - \frac{1}{2} \left(c_1^r + c_2^r + c_3^{r,1} \right) \right], \tag{5.18}$$

where the c_j^r ($j = 0, 1, 2$) and $c_3^{r,1}$ are given in (5.6a,b) and (5.16), the reduced Hamiltonian $\mathcal{H}_+^{(4)}$ takes the form

$$\mathcal{H}_+^{(4)} = \varepsilon^3 \frac{k_0^3(\omega_0 - \gamma)(\gamma^2 + 4\omega_0^2)}{8\pi\omega_0\Omega_0(2\omega_0 - \gamma)} \int U_1 U_2 \bar{U}_3 \bar{U}_4 \,\delta_{1+2-3-4} \,\mathrm{d}\lambda_{1234}$$

$$+ \varepsilon^4 \int \left(\frac{\beta}{8\pi}\,(\lambda_2 + \lambda_3) - \frac{k_0^2\omega_0^2}{4\pi\Omega_0^2}\,|\lambda_1 - \lambda_3| \right) U_1 U_2 \bar{U}_3 \bar{U}_4 \,\delta_{1+2-3-4}\,\mathrm{d}\lambda_{1234} + O(\varepsilon^5).$$

$$(5.19)$$

6. Hamiltonian Dysthe equation

The third-order normal form transformation eliminates all cubic terms from the Hamiltonian $\mathcal{H}$. In the modulational regime (5.1), the reduced Hamiltonian truncated at fourth order is

$$\mathcal{H} = \mathcal{H}^{(2)} + \mathcal{H}_+^{(4)}. \tag{6.1}$$

The goal now is to derive an associated Hamiltonian Dysthe equation for deep-water gravity waves with constant vorticity.

6.1. *Hamiltonian in the physical variables*

LEMMA 6.1. *In the physical variables* $(u, \bar{u})$, *the Hamiltonian* $\mathcal{H}$ *in* (6.1) *reads*

$$\mathcal{H} = \varepsilon \int \bar{u}\,\Omega\,(k_0 + \varepsilon D_X)u \,\mathrm{d}X + \varepsilon^3 \frac{k_0^3(\omega_0 - \gamma)(\gamma^2 + 4\omega_0^2)}{4\omega_0\Omega_0(2\omega_0 - \gamma)} \int |u|^4 \,\mathrm{d}X$$

$$+ \varepsilon^4 \frac{\beta}{2} \int |u|^2 \,\mathrm{Im}(\bar{u}\partial_X u) \,\mathrm{d}X - \varepsilon^4 \frac{k_0^2\omega_0^2}{2\Omega_0^2} \int |u|^2 \,|D_X|\,|u|^2 \,\mathrm{d}X + O(\varepsilon^5), \tag{6.2}$$

where $D_X = -\mathrm{i}\partial_X$ *in the slow spatial variable X.*

Proof. The first term in (6.2) comes out by applying the change of variables (5.2a,b) to the quadratic Hamiltonian

$$\mathcal{H}^{(2)} = \int \Omega\,(k_0 + \varepsilon\lambda)\,|z(k_0 + \varepsilon\lambda)|^2 \,\mathrm{d}k = \varepsilon \int \bar{u}\,\Omega\,(k_0 + \varepsilon D_X)u \,\mathrm{d}X, \tag{6.3}$$

where we use that $u(X) = (1/\sqrt{2\pi}) \int e^{\mathrm{i}\lambda X}\,U(\lambda)\,\mathrm{d}\lambda$ is the inverse Fourier transform of $U(\lambda)$. Furthermore,

$$\int U_1 U_2 \bar{U}_3 \bar{U}_4 \,\delta_{1+2-3-4} \,\mathrm{d}\lambda_{1234} = 2\pi \int |u|^4 \,\mathrm{d}X. \tag{6.4}$$

Similarly,

$$\int (\lambda_2 + \lambda_3) U_1 U_2 \bar{U}_3 \bar{U}_4 \,\delta_{1+2-3-4}\,\mathrm{d}\lambda_{1234} = 4\pi \int |u|^2 \,\mathrm{Im}(\bar{u}\partial_X u) \,\mathrm{d}X, \tag{6.5}$$

while the remaining term of $\mathcal{H}_+^{(4)}$ identifies to

$$\int |\lambda_1 - \lambda_3|\,U_1 U_2 \bar{U}_3 \bar{U}_4 \,\delta_{1+2-3-4}\,\mathrm{d}\lambda_{1234} = 2\pi \int |u|^2 \,|D_X|\,|u|^2 \,\mathrm{d}X. \tag{6.6}$$

∎

Expanding the linear dispersion relation in (6.2) around k_0 as

$$\Omega(k_0 + \varepsilon D_X) = \Omega_0 + \frac{gD_X}{2\omega_0}\,\varepsilon - \frac{g^2 D_X^2}{8\omega_0^3}\,\varepsilon^2 + \frac{g^3 D_X^3}{16\omega_0^5}\,\varepsilon^3 + O(\varepsilon^4) \tag{6.7}$$

gives an alternative form of the Hamiltonian $\mathcal{H}$ in the physical variables:

$$
\begin{aligned}
\mathcal{H} = \int \Bigg[&\varepsilon\,\Omega_0\,|u|^2 + \varepsilon^2\,\frac{g}{2\omega_0}\,\mathrm{Im}(\bar{u}\partial_X u) \\
&- \varepsilon^3\,\frac{g^2}{8\omega_0^3}\,|\partial_X u|^2 + \varepsilon^3\,\frac{k_0^3(\omega_0 - \gamma)(\gamma^2 + 4\omega_0^2)}{4\omega_0\Omega_0(2\omega_0 - \gamma)}\,|u|^4 - \varepsilon^4\,\frac{g^3}{16\omega_0^5}\,\mathrm{Im}(\bar{u}\partial_X^3 u) \\
&+ \varepsilon^4\,\frac{\beta}{2}\,|u|^2\,\mathrm{Im}(\bar{u}\partial_X u) - \varepsilon^4\,\frac{k_0^2\omega_0^2}{2\Omega_0^2}\,|u|^2|D_X|\,|u|^2 \Bigg]\,\mathrm{d}X + O(\varepsilon^5).
\end{aligned}
\tag{6.8}
$$

6.2. *Derivation of the Dysthe equation*

Using the relation (5.3) rewritten as

$$\begin{pmatrix} u \\ \bar{u} \end{pmatrix} = P_2 \begin{pmatrix} z \\ \bar{z} \end{pmatrix} = \varepsilon^{-1} \begin{pmatrix} \mathrm{e}^{-\mathrm{i}k_0 x} & 0 \\ 0 & \mathrm{e}^{\mathrm{i}k_0 x} \end{pmatrix} \begin{pmatrix} z \\ \bar{z} \end{pmatrix}, \tag{6.9}$$

the Hamiltonian system (2.32) takes the form

$$\partial_t \begin{pmatrix} u \\ \bar{u} \end{pmatrix} = J_2 \begin{pmatrix} \partial_u \mathcal{H} \\ \partial_{\bar{u}} \mathcal{H} \end{pmatrix} = \varepsilon^{-1} \begin{pmatrix} 0 & -\mathrm{i} \\ \mathrm{i} & 0 \end{pmatrix} \begin{pmatrix} \partial_u \mathcal{H} \\ \partial_{\bar{u}} \mathcal{H} \end{pmatrix}, \tag{6.10}$$

where $J_2 = \varepsilon P_2 J_1 P_2^*$ (Craig, Guyenne & Sulem 2010). The additional factor ε in the definition of J_2 reflects the change in symplectic structure associated with the spatial rescaling $X = \varepsilon x$.

Substituting the reduced Hamiltonian (6.8) into (6.10), we get

$$
\begin{aligned}
\mathrm{i}\,\partial_t u &= \varepsilon^{-1}\partial_{\bar{u}}\mathcal{H} \\
&= \Omega_0 u - \mathrm{i}\varepsilon\,\frac{g}{2\omega_0}\,\partial_X u + \varepsilon^2\,\frac{g^2}{8\omega_0^3}\,\partial_X^2 u + \varepsilon^2\,\frac{k_0^3(\omega_0 - \gamma)(\gamma^2 + 4\omega_0^2)}{2\omega_0\Omega_0(2\omega_0 - \gamma)}\,|u|^2 u \\
&\quad + \mathrm{i}\varepsilon^3\,\frac{g^3}{16\omega_0^5}\,\partial_X^3 u - \mathrm{i}\varepsilon^3\beta\,|u|^2\,\partial_X u - \varepsilon^3\,\frac{k_0^2\omega_0^2}{\Omega_0^2}\,u\,|D_X|\,|u|^2,
\end{aligned}
\tag{6.11}
$$

which is a Hamiltonian Dysthe equation for two-dimensional gravity waves on deep water with constant vorticity. It describes modulated waves moving in the positive *x*-direction at group velocity $\Omega_0' = \partial_k\Omega(k_0) = g/(2\omega_0)$ as indicated by the advection term. The non-local term $u\,|D_X|\,|u|^2$ is a signature of the Dysthe equation, which reflects the presence of the wave-induced mean flow. The coefficient β is given by (5.18). The coefficient of the nonlinear term $|u|^2 u$ above agrees with that in the NLS equation of Thomas *et al.* (2012) and in the Dysthe equation of Curtis *et al.* (2018) (see (7.15) below) up to scaling factors consistent with the difference in definition for the wave envelope described in the various models.

The first two terms on the right-hand side of (6.11) can be eliminated via phase invariance and reduction to a moving reference frame. The latter is equivalent, in the

949 A50-24

framework of canonical transformations, to subtraction from $\mathcal{H}$ of a multiple of the momentum (2.19), which reduces to

$$I = \int \eta \, \partial_x \zeta \, \mathrm{d}x = \varepsilon \int \left[k_0 \, |u|^2 + \varepsilon \, \mathrm{Im}(\bar{u} \, \partial_X u) \right] \mathrm{d}X, \tag{6.12}$$

while the former is equivalent to subtraction from $\mathcal{H}$ of a multiple of the wave action

$$M = \varepsilon \int |u|^2 \, \mathrm{d}X, \tag{6.13}$$

which is conserved due to the phase-invariance property of the Dysthe equation. Because I and M Poisson commute with $\mathcal{H}$, this transformation preserves the symplectic structure J_2 (Craig *et al.* 2021*b*). The resulting Hamiltonian is given by

$$\hat{\mathcal{H}} = \mathcal{H} - \Omega_0' I - \left(\Omega_0 - k_0 \Omega_0' \right) M, \tag{6.14}$$

which, after introducing a new long-time scale $\tau = \varepsilon^2 t$, leads to the following version of the Hamiltonian Dysthe equation:

$$\mathrm{i} \, \partial_\tau u = \frac{g^2}{8\omega_0^3} \partial_X^2 u + \frac{k_0^3(\omega_0 - \gamma)(\gamma^2 + 4\omega_0^2)}{2\omega_0 \Omega_0 (2\omega_0 - \gamma)} \, |u|^2 u + \mathrm{i}\varepsilon \, \frac{g^3}{16\omega_0^5} \, \partial_X^3 u$$

$$- \mathrm{i}\varepsilon\beta \, |u|^2 \, \partial_X u - \varepsilon \, \frac{k_0^2 \omega_0^2}{\Omega_0^2} \, u \, |D_X| \, |u|^2. \tag{6.15}$$

This governs the long-time evolution of the envelope of modulated waves in a reference frame moving in the positive horizontal direction at group velocity Ω_0'. The non-local operator $|D_X|$ is the Fourier multiplier with symbol $|\lambda|$. The associated Hamiltonian reads more explicitly (after multiplying by ε^{-3} and dropping the hat)

$$\mathcal{H} = \int \left[-\frac{g^2}{8\omega_0^3} \, |\partial_X u|^2 + \frac{k_0^3(\omega_0 - \gamma)(\gamma^2 + 4\omega_0^2)}{4\omega_0 \Omega_0 (2\omega_0 - \gamma)} \, |u|^4 - \varepsilon \, \frac{g^3}{16\omega_0^5} \, \mathrm{Im}(\bar{u} \, \partial_X^3 u) \right.$$

$$\left. + \varepsilon \, \frac{\beta}{2} \, |u|^2 \, \mathrm{Im}(\bar{u} \, \partial_X u) - \varepsilon \, \frac{k_0^2 \omega_0^2}{2\Omega_0^2} \, |u|^2 \, |D_X| \, |u|^2 \right] \mathrm{d}X. \tag{6.16}$$

As suggested by Trulsen *et al.* (2000), retaining the exact linear dispersion relation, rather than expanding it in powers of ε, may provide an overall better approximation of the wave envelope. On a related note, Obrecht & Saut (2015) proposed a full-dispersion Davey–Stewartson system and compared its analytical properties to those of the classical version. In the present context, the Dysthe equation with full linear dispersion takes the form

$$\mathrm{i} \, \partial_t u = \Omega \, (k_0 + \varepsilon D_X) u + \varepsilon^2 \, \frac{k_0^3(\omega_0 - \gamma)(\gamma^2 + 4\omega_0^2)}{2\omega_0 \Omega_0 (2\omega_0 - \gamma)} \, |u|^2 u$$

$$- \mathrm{i}\varepsilon^3 \beta \, |u|^2 \, \partial_X u - \varepsilon^3 \, \frac{k_0^2 \omega_0^2}{\Omega_0^2} \, u \, |D_X| \, |u|^2, \tag{6.17}$$

and the corresponding Hamiltonian is given by (6.2).

7. Numerical results

We now present numerical simulations to illustrate the performance of our Hamiltonian Dysthe equation. We consider the problem of modulational stability of Stokes waves and examine the influence of vorticity. We compare these results to predictions by another related envelope model and to direct simulations of the full nonlinear equations. We also test the capability of our reconstruction procedure against a simpler approach.

7.1. *Stability of Stokes waves*

We first give the theoretical prediction for modulational or Benjamin–Feir (BF) instability of Stokes waves. These are represented by the exact uniform solution

$$u_0(t) = B_0 \exp(-\mathrm{i}(\Omega_0 + \varepsilon^2 \beta_0 B_0^2)t), \tag{7.1}$$

for (6.11), where B_0 is a positive real constant, and

$$\beta_0 = \frac{k_0^3(\omega_0 - \gamma)(\gamma^2 + 4\omega_0^2)}{2\omega_0 \Omega_0 (2\omega_0 - \gamma)}. \tag{7.2}$$

In the irrotational case ($\gamma = 0$), such a solution is known to be linearly unstable with respect to sideband (i.e. long-wave) perturbations.

The formal calculation consists in linearizing (6.11) about u_0 by inserting a perturbation of the form

$$u(X, t) = u_0(t) \left[1 + B(X, t) \right], \tag{7.3}$$

where

$$B(X, t) = B_1 \exp(\sigma t + \mathrm{i}\lambda X) + B_2 \exp(\bar{\sigma} t - \mathrm{i}\lambda X), \tag{7.4}$$

and B_1, B_2 are complex coefficients. We find that the condition $\mathrm{Re}(\sigma) \neq 0$ for instability implies

$$\alpha = \frac{g^2}{8\omega_0^3} \lambda^2 \Gamma > 0, \tag{7.5}$$

with

$$\Gamma = 2B_0^2 (\beta_0 - \varepsilon\beta_3 |\lambda|) - \frac{g^2}{8\omega_0^3} \lambda^2, \quad \beta_3 = \frac{k_0^2 \omega_0^2}{\Omega_0^2}. \tag{7.6a,b}$$

This is a tedious but straightforward calculation, for which we skip the details. Similar calculations can be found in Curtis *et al.* (2018), Dysthe (1979) and Gramstad & Trulsen (2011).

Figure 1 depicts the normalized growth rate

$$\frac{|\mathrm{Re}(\sigma)|}{\omega_0} = \frac{\sqrt{\alpha}}{\omega_0}, \tag{7.7}$$

delimiting the instability region as predicted by condition (7.5) for $(B_0, k_0) = (0.002, 10)$ and various values of γ. The growth rate (and instability region) for $\gamma = 0$ is also included as a reference. Hereafter, all the variables are rescaled to absorb ε back into their definition, and all the equations are non-dimensionalized by using $1/k_0$ and $1/\sqrt{gk_0}$ as characteristic length and time scales, respectively, so that $g = 1$. For convenience, we retain the same
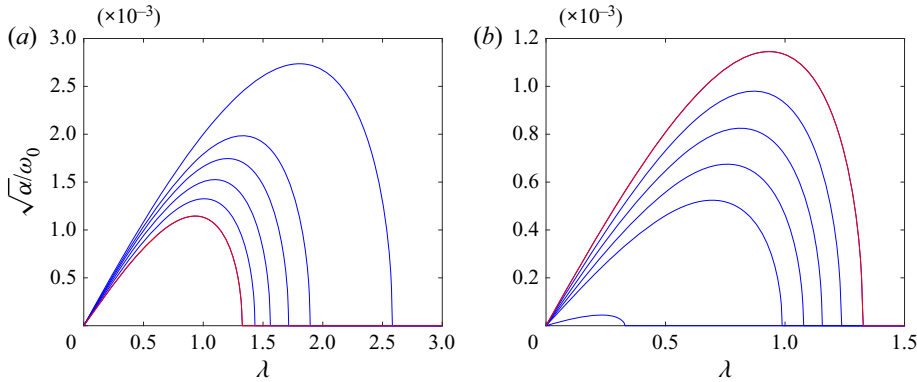
949 A50-26

Figure 1. Regions of modulational instability according to (7.5) for $(B_0, k_0) = (0.002, 10)$. The blue curves correspond to $\gamma \neq 0$, while the red curve corresponds to $\gamma = 0$: (*a*) $\gamma = \{-0.5, -1, -1.5, -2, -3.5\}$ (expanding curves with decreasing γ); (*b*) $\gamma = \{+0.5, +1, +1.5, +2, +3.5\}$ (shrinking curves with increasing γ).

notations for all the dimensionless quantities. We set $\varepsilon = k_0 A_0$ (surface wave steepness), noting that the envelope amplitude B_0 and the surface amplitude A_0 are related via

$$B_0 = A_0 \sqrt{\frac{\omega_0}{2k_0}}, \tag{7.8}$$

according to (2.31) and (5.3). The graphs in figure 1 correspond to a wave steepness of about $\varepsilon = 0.05$. Clearly, the vorticity γ (both its magnitude and sign) has an influence on (7.5). We see that $\gamma < 0$ tends to enhance the instability by amplifying the growth rate and enlarging the instability region to higher sideband wavenumbers. On the other hand, $\gamma > 0$ tends to diminish it. Figure 1 even suggests that for sufficiently large $\gamma > 0$, instability no longer occurs. This is confirmed by figure 2, which shows that the factor Γ in (7.5) is no longer positive at any wavenumber λ when $\gamma > 3.5$ for $(B_0, k_0) = (0.002, 10)$. A positive vorticity (co-propagating current) therefore has a stabilizing effect on the dynamics of Stokes waves.

7.2. *Reconstruction of the original variables*

At any instant t, the surface elevation and velocity potential can be reconstructed from the wave envelope by inverting the normal form transformation. This is accomplished by solving the auxiliary system (3.37)–(3.38) backward from $s = 0$ to $s = -1$, with 'initial' conditions given by the transformed variables

$$\eta(x, t)|_{s=0} = \frac{1}{\sqrt{2}} \, a^{-1}(D) \left[u(x, t) \, e^{ik_0 x} + \bar{u}(x, t) \, e^{-ik_0 x} \right], \tag{7.9}$$

$$\zeta(x, t)|_{s=0} = \frac{1}{i\sqrt{2}} \, a(D) \left[u(x, t) \, e^{ik_0 x} - \bar{u}(x, t) \, e^{-ik_0 x} \right], \tag{7.10}$$

according to (2.35*a*,*b*) and (5.3). In these expressions, u obeys (6.11) and $a^{-1}(D) = \sqrt{|D|/\omega(D)}$. The final solution at $s = -1$ represents the original variables (η, ζ). Starting from the first harmonics (with carrier wavenumber k_0) in the initial conditions (7.9)–(7.10), the evolutionary process in s will generate automatically the next-order contributions from
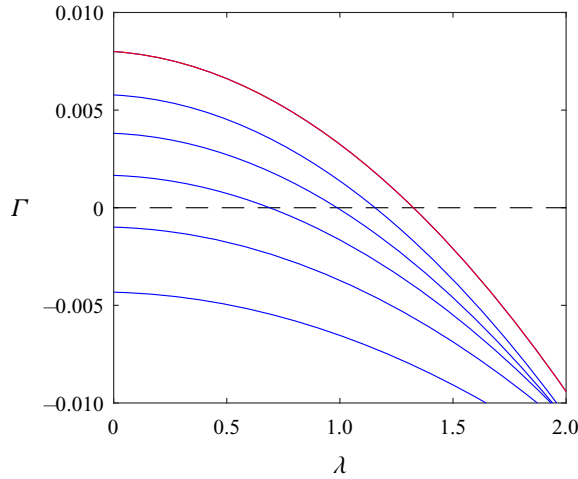
Figure 2. Plots of Γ versus λ for $(B_0, k_0) = (0.002, 10)$ and $\gamma = \{0, +1, +2, +3, +4, +5\}$ (falling curves with increasing γ). The red curve corresponds to $\gamma = 0$.

lower and higher harmonics via nonlinear interactions according to (3.37)–(3.38). Recall also that the non-canonical velocity potential ξ can be recovered from the canonical one ζ via the direct relation (2.20).

7.3. *Simulations and comparisons*

For the comparison, the full nonlinear system (2.15) is solved numerically following a high-order spectral approach (Craig & Sulem 1993). The corresponding equations read more explicitly

$$\partial_t \eta = G(\eta)\,\xi + \gamma\,\eta\,\partial_x \eta, \tag{7.11}$$

$$\partial_t \xi = -g\eta - \frac{1}{2}\,(\partial_x \xi)^2 + \frac{1}{2}\,\frac{[G(\eta)\,\xi + (\partial_x \eta)(\partial_x \xi)]^2}{1 + (\partial_x \eta)^2} + \gamma\,\eta\,\partial_x \xi + \gamma\,\partial_x^{-1} G(\eta)\,\xi. \tag{7.12}$$

These are discretized in space by a pseudo-spectral method based on the fast Fourier transform (FFT). The computational domain is taken to be $0 \leqslant x \leqslant 2\pi$ with periodic boundary conditions, and is divided into a regular mesh of N collocation points. The Dirichlet–Neumann operator is computed via its series expansion (2.26) for which a small number m of terms is sufficient to achieve highly accurate results by virtue of its analyticity properties. The value $m = 6$ is selected based on previous extensive tests (Xu & Guyenne 2009). Time integration of (7.11) and (7.12) is carried out in the Fourier space so that linear terms can be solved exactly by the integrating factor technique. The nonlinear terms are integrated in time by using a fourth-order Runge–Kutta scheme with constant step Δt. More details can be found in Guyenne (2017, 2018).

The same numerical methods are applied to the envelope equation (6.11), as well as to the reconstruction procedure, with the same resolutions in space and time. In particular, the auxiliary system (3.37)–(3.38) is integrated in s by using the same step size $\Delta s = \Delta t$. While this system of equations may look complicated, its numerical treatment is straightforward and efficient via the FFT. Moreover, because this computation is not performed at each instant t (only when data on η are required), and because it is performed over a short interval $-1 \leqslant s \leqslant 0$, the associated cost is insignificant. Note that by virtue
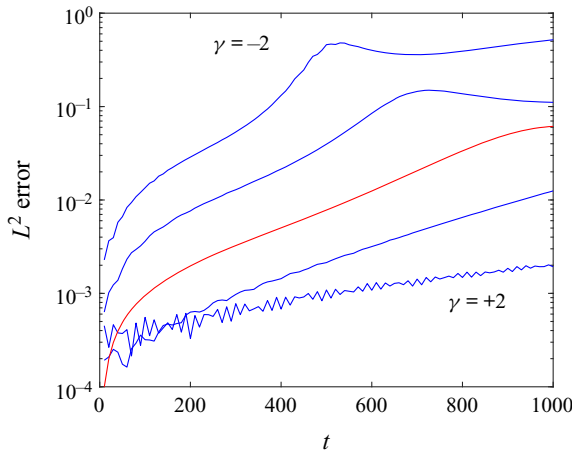
Figure 3. Relative L^2 errors on η between fully and weakly nonlinear solutions for $(B_0, k_0, \lambda) = (0.002, 10, 1)$ and $\gamma = \{-2, -1, 0, +1, +2\}$. The red curve corresponds to $\gamma = 0$.

of the zero-mass assumption (2.25), indetermination at $k = 0$ in the evaluation of any quantity involving a Fourier multiplier such as ∂_x^{-1} or $|D|^{-1}$ may be lifted by simply setting its zeroth-mode component to zero.

To examine the stability of Stokes waves in the presence of a shear current, initial conditions of the form

$$u(x, 0) = B_0 \left[1 + 0.1 \cos(\lambda x)\right] \tag{7.13}$$

are specified for (6.11), where λ denotes the wavenumber of some long-wave perturbation. For the purpose of comparing with the full system (7.11)–(7.12), initial conditions $\eta(x, 0)$ and $\xi(x, 0)$ are reconstructed by solving (3.37)–(3.38) from transformed initial data (7.9)–(7.10) given in terms of (7.13).

The following tests focus on the case $(B_0, k_0, \lambda) = (0.002, 10, 1)$ as considered in the previous stability analysis. The spatial and temporal resolutions are set to $\Delta x = 0.012$ ($N = 512$) and $\Delta t = 0.005$. Figure 3 shows the time evolution of the relative L^2 error

$$\frac{\|\eta_f - \eta_w\|_2}{\|\eta_f\|_2} \tag{7.14}$$

on η between the fully (η_f) and weakly (η_w) nonlinear solutions, for various values of $\gamma \lessgtr 0$. We see that the errors remain under unity (i.e. under 100 %) over the time interval $0 \leqslant t \leqslant 1000$, noting that the validity of the Dysthe equation deteriorates faster as γ is decreased. This is expected in view of the stability analysis because the solution tends to become more unstable (and thus more nonlinear) with decreasing γ. Development of the BF instability is especially apparent for $\gamma = -1$ and -2, as indicated by a hump in their error plots.

Comparison of surface elevations η predicted from the weakly nonlinear equation (6.11) and the full nonlinear system (7.11)–(7.12) is presented in figure 4 for the same set of values of γ at their respective times of maximum wave growth. The perturbed Stokes wave at $t = 0$ (which is the same initial condition for all cases considered) is depicted in figure 4(*a*). These results are consistent with our previous observations from figures 1 and 3. Excitation and growth of the most unstable sideband mode $\lambda = 1$ (according to the stability analysis) are clearly revealed in these plots. A more negative γ promotes the BF instability (by making it happen sooner with a stronger wave amplification), while a more
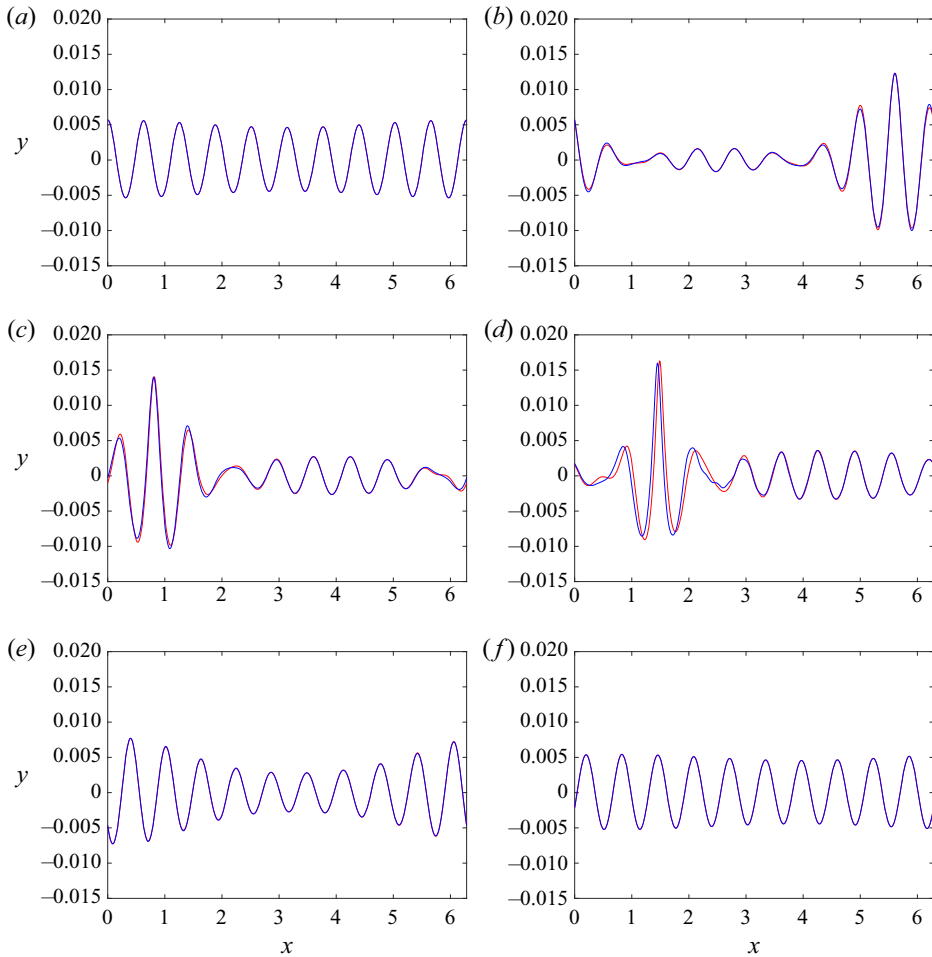
Figure 4. Comparison of surface elevations η between fully and weakly nonlinear solutions for $(B_0, k_0, \lambda) = (0.002, 10, 1)$ with (*a*) $\gamma = 0$ ($t = 0$), (*b*) $\gamma = 0$ ($t = 940$), (*c*) $\gamma = -1$ ($t = 680$), (*d*) $\gamma = -2$ ($t = 500$), (*e*) $\gamma = +1$ ($t = 1000$), (*f*) $\gamma = +2$ ($t = 1000$). The blue curve represents the Hamiltonian Dysthe equation, while the red curve represents the full nonlinear system.

positive γ tends to reduce and even offset it. In all these cases, the Dysthe model is found to provide a very good approximation up to at least $t = 1000$. As expected, for $\gamma = -2$, discrepancies are more pronounced due to the higher nonlinearity reached; a slight phase lag and drop in wave amplitude can be discerned around the main peak at $t = 500$.

It is suitable to compare our Hamiltonian Dysthe equation (6.11) with another related model that has recently been derived by Curtis *et al.* (2018) and Curtis & Murphy (2020) in the same physical setting. Note that these authors additionally considered surface tension, but we will only examine the gravity wave version of their model. Moreover, because they expressed their model in a form that contains a first derivative in time as well as a mixed derivative in space and time (see (2.37) in Curtis *et al.* 2018), we find it more appropriate to rewrite it in a more standard form with a single time derivative (as it is typically so for the Dysthe equation; Dysthe 1979) to allow for a fairer comparison. We also take into account the fact that vorticity in the mathematical formulation used by Curtis *et al.* (2018) is defined as the opposite of ours. The resulting model for the first-harmonic envelope η_1

is given by

$$\partial_t \eta_1 = -c_g\,\partial_x\eta_1 - i\,\frac{c_g^2}{d_0}\,\partial_x^2\eta_1 + 2\,\frac{c_g^3}{d_0^2}\,\partial_x^3\eta_1 - i\,\frac{\tilde{\alpha}_0}{d_0}\,|\eta_1|^2\eta_1$$

$$- \frac{\tilde{\alpha}_1}{d_0}\,|\eta_1|^2\,\partial_x\eta_1 - \frac{\tilde{\alpha}_2}{d_0}\,\eta_1^2\,\partial_x\bar{\eta}_1 + i\,\frac{\tilde{\alpha}_3}{d_0}\,\eta_1 H\,\partial_x|\eta_1|^2\,, \qquad (7.15)$$

where

$$\left.\begin{array}{c} d_0 = 2\Omega_0 - \gamma, \quad c_g = \dfrac{1}{d_0}, \quad d_1 = \dfrac{d_0}{1+\gamma c_g}, \quad \tilde{\alpha}_0 = \alpha_0 - \gamma^2 k_0 d_0 d_1, \\[2mm] \tilde{\alpha}_1 = \alpha_1 - \gamma^2 k_0 d_1(c_g + \alpha_d\gamma d_1) - \gamma^2 d_1(2d_0 + 3k_0 c_g) + 4c_g(\gamma^2 k_0 d_1 - \alpha_0 c_g), \\[2mm] \tilde{\alpha}_2 = \alpha_2 + \gamma^2 k_0 d_1(c_g + \alpha_d\gamma d_1) - \gamma^2 d_1(d_0 + k_0 c_g) + 2c_g(\gamma^2 k_0 d_1 - \alpha_0 c_g), \\[2mm] \tilde{\alpha}_3 = \alpha_3 - \gamma k_0 c_g d_1(d_0 + d_1). \end{array}\right\} \tag{7.16}$$

The reader is directed to Curtis *et al.* (2018), where the expressions for α_d and α_j ($j = 0,\ldots,3$) can be found. Note that $H\,\partial_x = |D|$ for the non-local term in (7.15). For the purpose of comparing with the full system (7.11)–(7.12), we have also re-expressed the Curtis *et al.* model in a fixed reference frame, hence the additional advection term in (7.15) as compared to (2.37) in Curtis *et al.* (2018). In the following discussion, we will refer to (7.15) as the 'classical' Dysthe equation for this problem, because it is not Hamiltonian and has the same typical form as in the irrotational case. Furthermore, its derivation is based on a perturbative Stokes-type expansion for the dependent variables η and ξ, which is similar to the classical derivation by the method of multiple scales (Dysthe 1979). Indeed, following Curtis *et al.* (2018), the surface elevation and velocity potential at any instant t can be reconstructed perturbatively from η_1 as

$$\left.\begin{array}{c} \eta(x,t) = \gamma d_1\,|\eta_1|^2 + 2\,\mathrm{Re}\left(\eta_1\,e^{i\theta} + \ell_0\eta_1^2\,e^{2i\theta} + \cdots\right), \\[3mm] \xi(x,t) = H\left(\dfrac{\Omega_0}{k_0}\,\eta - \dfrac{\Omega_0}{k_0}\,\eta H\,\partial_x\eta - \dfrac{\gamma}{2}\,\eta^2 + \dfrac{\Omega_0}{2k_0}\,H\,\partial_x(\eta^2) + \cdots\right), \end{array}\right\} \tag{7.17}$$

for which the expression of ℓ_0 can be found in Curtis *et al.* (2018), and only contributions from up to the second harmonics are included here because Curtis *et al.* (2018) did not provide expressions for contributions from higher harmonics. The phase function is given by $\theta = k_0 x - \Omega_0 t$. The 'classical' reconstruction procedure based on (7.17) clearly differs from the present approach. It is more explicit and thus computationally more efficient, but it is perturbative. Contributions at each order up to the desired one need to be derived, and their expressions become increasingly complicated. On the other hand, our Hamiltonian procedure requires solving an auxiliary system of PDEs to reconstruct η and ζ (or ξ) from u, but it is non-perturbative. Indeed, (3.37) and (3.38) constitute an exact representation of the Birkhoff normal form transformation that eliminates non-resonant triads in this problem.

As an illustration, figure 5 compares the L^2 errors (7.14) on η from the classical and Hamiltonian Dysthe equations in the large-vorticity cases $\gamma = \pm 2$. For each of these models, the error is calculated relative to the fully nonlinear solution with respective initial
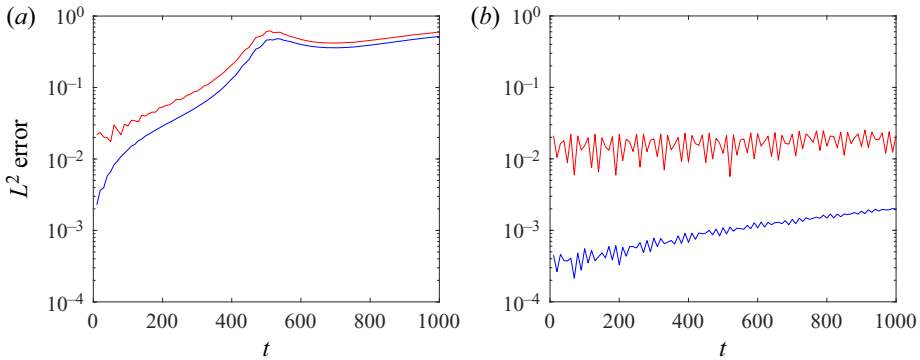
Figure 5. Relative L^2 errors on η between fully and weakly nonlinear solutions for $(B_0, k_0, \lambda) = (0.002, 10, 1)$. The blue curve represents the Hamiltonian Dysthe equation, while the red curve represents the classical Dysthe equation: (a) $\gamma = -2$, (b) $\gamma = +2$.

conditions $\eta(x, 0)$ and $\xi(x, 0)$. These are provided by (7.17) with

$$\eta_1(x, 0) = \frac{A_0}{2} [1 + 0.1 \cos(\lambda x)] \tag{7.18}$$

when (7.15) is tested against (7.11)–(7.12). Recall that A_0 and B_0 are related through (7.8). We use the same numerical methods as described earlier (and specify the same resolutions in space and time) to solve (7.15) and evaluate (7.17). For $\gamma = -2$, both Dysthe solutions are found to perform similarly, with the error from the Hamiltonian model being slightly lower than that from the classical model. The relatively quick loss of accuracy in this case, which is common to both models (with errors reaching near 50 % at $t \simeq 500$) should be attributed to deterioration of the Dysthe approximation during development of the BF instability, rather than to the reconstruction procedure. By contrast, for $\gamma = +2$, the errors remain small and do not vary much over the time interval $0 \leqslant t \leqslant 1000$, which is expected considering that the solution is more stable in this case. We see, however, that the present approach outperforms the classical one by about an order of magnitude. In all these error plots, the seemingly sharp values near $t = 0$ are already an indication of the level of approximation associated with the different equations, as they represent adjustment of the full system (7.11)–(7.12) to the imposed initial conditions during early stages of the simulation.

The corresponding surface profiles are depicted in figure 6 for the unstable case $\gamma = -2$, with predictions from each Dysthe model being compared to the fully nonlinear solution. Snapshots of η at $t = 390$ (early stage of BF instability), $t = 500$ (around the time of maximum wave growth) and $t = 1000$ (near the end of the quasi-recurrent cycle of modulation–demodulation) are presented. The satisfactory performance of both Dysthe solutions as indicated in this figure is consistent with the error plots in figure 5. A noticeable discrepancy between the weakly and fully nonlinear predictions is a phase lag that tends to develop over time. Otherwise, salient features of the wave dynamics (including the shape of the steep wave at $t = 500$) seem to be well captured, even in this highly focusing regime. Regarding the comparison of surface profiles for $\gamma = +2$, these look indistinguishable from figure 4(f) at the graphical scale and thus are not displayed for convenience.

We point out in passing that the main purpose of these tests is not to show whether one modulational approach is better than the other. In particular, regarding the reconstruction procedure for the classical Dysthe equation, we understand that adding contributions from
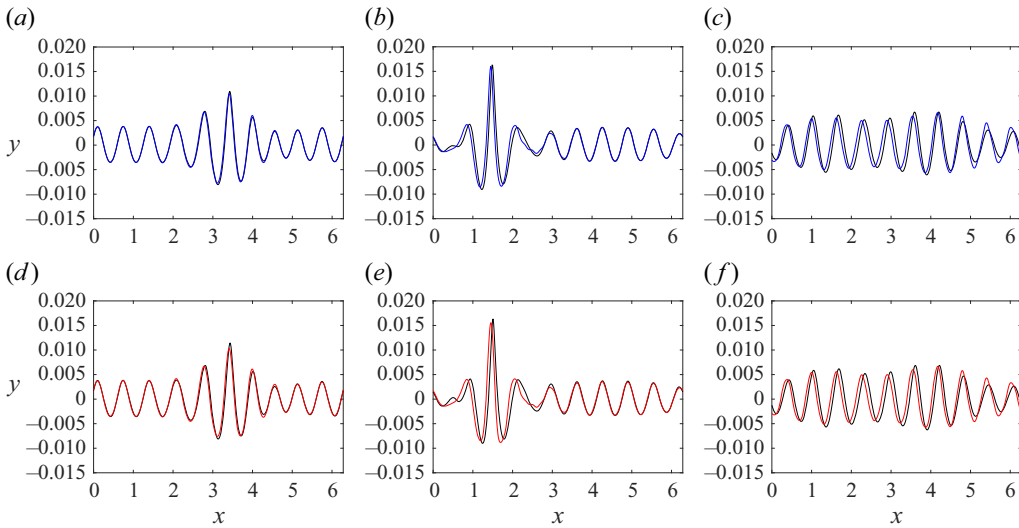
Figure 6. Comparison on η between fully and weakly nonlinear solutions for $(B_0, k_0, \lambda) = (0.002, 10, 1)$ and $\gamma = -2$ at $t = 390, 500, 1000$ (from left to right). $(a–c)$ Hamiltonian Dysthe equation in blue; $(d–f)$ classical Dysthe equation in red. The black curve represents the full nonlinear system.

higher harmonics to formulas (7.17) would likely improve their accuracy and lead to closer agreement with the full system. Rather, a goal here is to validate our new Hamiltonian approach against other existing formulations. As a byproduct of this comparison, given the overall positive assessment based on figures 5 and 6, we in turn provide an independent validation of the Curtis *et al.* model. Such a validation was not conducted in their earlier study (Curtis *et al.* 2018; Curtis & Murphy 2020).

It is comforting to see that the solution of (3.37)–(3.38) helps to achieve an accurate computation of the free surface in our Hamiltonian framework, which was not obvious considering the rather lengthy expressions of (3.37)–(3.38). The good agreement found also confirms the validity of the zero-mass assumption (2.25) since it is used to evaluate non-local terms in (3.37)–(3.38). To further demonstrate the effectiveness of this reconstruction scheme (which we will refer to as full reconstruction by solving (3.37)–(3.38)), we now test the Hamiltonian Dysthe equation (6.11) by simply using (7.9)–(7.10) to recover η and ζ from u at any instant t (which we will refer to as partial reconstruction). This simplified procedure is equivalent to retaining only contributions from the first harmonics in the representation of η and ζ.

The L^2 errors (7.14) associated with these two versions of our Hamiltonian approach are illustrated in figure 7 for $\gamma = \pm 2$. We have made sure again that suitable initial conditions are specified for the full system (7.11)–(7.12) when comparing it to each version. These results confirm that the decline in performance (for partial versus full reconstruction of η) can be considerable. The difference is found to be by about an order of magnitude for $\gamma = -2$, and by more than two orders of magnitude for $\gamma = +2$. In both cases, the errors grow quickly to exceed 100 % at some point during the time interval $0 \leqslant t \leqslant 1000$.

Examination of the surface profiles obtained from partial reconstruction as compared to the fully nonlinear solution is provided in figure 8 for $\gamma = \pm 2$. Consistent with the error plots in figure 7, we see that the discrepancies in wave amplitude and phase tend to develop faster. The phase lag is clearly noticeable and affects the entire wave train, even in
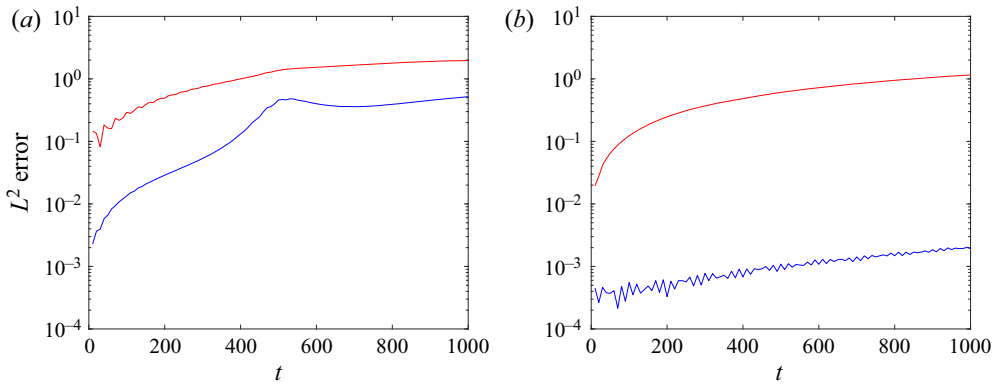
Figure 7. Relative L^2 errors on η between fully and weakly nonlinear solutions for $(B_0, k_0, \lambda) = (0.002, 10, 1)$. The blue curve represents the Hamiltonian Dysthe equation with full reconstruction, while the red curve represents the Hamiltonian Dysthe equation with partial reconstruction: (a) $\gamma = -2$, (b) $\gamma = +2$.
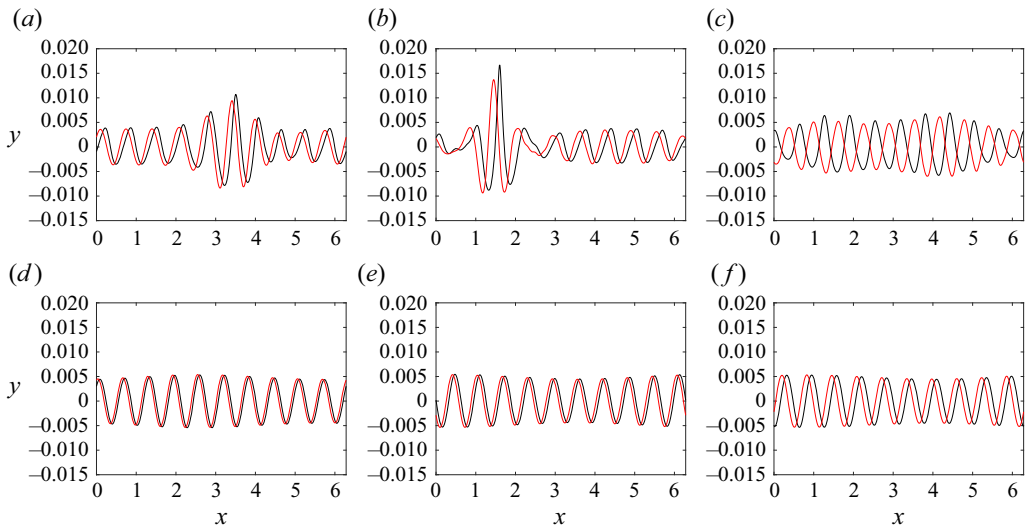

Figure 8. Comparison on η between fully and weakly nonlinear solutions for $(B_0, k_0, \lambda) = (0.002, 10, 1)$ at $t = 390, 500, 1000$ (from left to right). The red curve represents the Hamiltonian Dysthe equation with partial reconstruction, while the black curve represents the full nonlinear system: (a–c) $\gamma = -2$, (d–f) $\gamma = +2$.

the stabilizing case $\gamma = +2$. It is so severe for $\gamma = -2$ that the weakly nonlinear solution appears completely out of phase at $t = 1000$ during the near-recurrent stage.

Finally, the time evolution of the relative error

$$\frac{\Delta \mathcal{H}}{\mathcal{H}_0} = \frac{|\mathcal{H} - \mathcal{H}_0|}{\mathcal{H}_0} \tag{7.19}$$

on energy (6.8) and on wave action (6.13) associated with the Hamiltonian Dysthe equation (6.11) is shown in figure 9 for various values of γ. Integrals in (6.8) and in the L^2 norm (7.14) are computed via the trapezoidal rule over the periodic cell $[0, 2\pi]$. The reference value $\mathcal{H}_0$ denotes the initial value of (6.8) at $t = 0$. Overall, $\mathcal{H}$ is very well conserved in all these cases. The gradual loss of accuracy over time, which becomes more pronounced
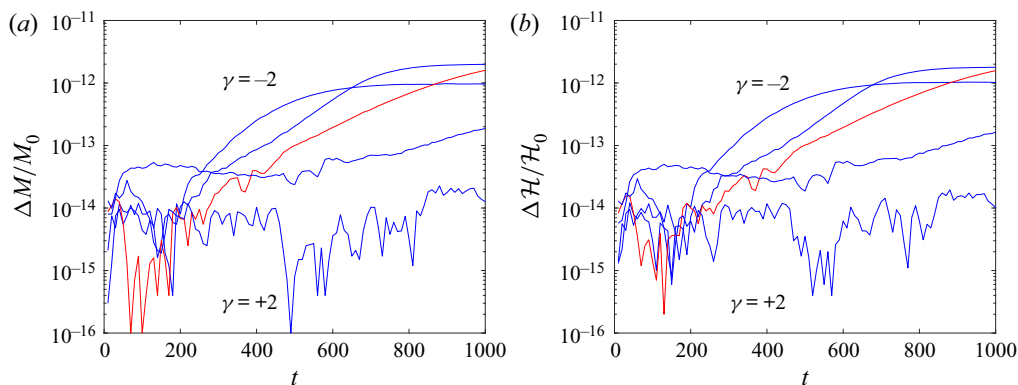
949 A50-34

Figure 9. Relative errors on (*a*) M and (*b*) $\mathcal{H}$ for the Hamiltonian Dysthe equation with $(B_0, k_0, \lambda) = (0.002, 10, 1)$ and $\gamma = \{-2, -1, 0, +1, +2\}$. The red curve corresponds to $\gamma = 0$.

as γ is decreased, is likely due to amplification of numerical errors triggered by the BF instability.

8. Conclusion

Starting from the basic Hamiltonian formulation of the water wave problem with constant vorticity as proposed by Wahlén (2007) and Constantin *et al.* (2008), we derive a Hamiltonian version of the Dysthe equation (a higher-order NLS equation) for the nonlinear modulation of two-dimensional gravity waves on deep water, in the presence of a background uniform shear flow. The resulting model exhibits a well-defined symplectic structure and conserves an energy (i.e. the reduced Hamiltonian) over time. Our methodology, introduced recently for two- and three-dimensional irrotational gravity waves (Craig *et al.* 2021*a*; Guyenne *et al.* 2021, 2022), consists in performing a sequence of canonical transformations that involve a reduction to normal form (devoid of non-resonant triads) and use of a modulational ansatz together with a scale separation lemma. A novelty of our approach is a direct reconstruction of the surface variables from the wave envelope through inversion of the third-order normal form transformation. This reconstruction requires solving an auxiliary Hamiltonian system of PDEs, for which we provide an explicit derivation. Such a procedure differs from the classical one where physical quantities like the surface elevation are reconstructed perturbatively in terms of a Stokes expansion. As a consequence, both steps (solving for the wave envelope and recovering the surface elevation) fit consistently within a Hamiltonian framework.

To validate our approximation, we perform numerical simulations of this Hamiltonian Dysthe equation and compare them to computations based on the full water wave system and another related Dysthe equation recently derived by Curtis *et al.* (2018) in the same setting. For a range of values of the vorticity, we examine the long-time dynamics of perturbed Stokes waves and find very good agreement, thus providing a verification for both Dysthe models. In particular, the performance of our Hamiltonian model is found to be quite satisfactory over the entire range considered. We observe that the presence of vorticity clearly has an effect on the BF instability of Stokes waves on deep water. Consistent with results from previous studies, a counter-propagating shear flow (negative vorticity) tends to enhance this instability as it amplifies the growth rate and enlarges the instability region to higher sideband wavenumbers, while a co-propagating current (positive vorticity) tends to stabilize it. We hope that this Hamiltonian Dysthe equation

may serve as an efficient tool to study wave–current interactions in future applications. As subsequent work, it would be of interest to extend the present method to the situation of constant finite depth with possibly surface tension. For this problem, the reduction to normal form is expected to be significantly more complicated.

While the problem under consideration for water waves in the presence of constant vorticity is inherently two-dimensional, we point out that the Hamiltonian perturbation method being advocated here to examine this problem is extensible to three dimensions (Craig *et al.* 2010, 2021*b*). In particular, this approach may be used to investigate short-crested waves as observed in the irrotational case. Approximations to such waves have been obtained e.g. via reduced models based on the Zakharov equation with a focus on crescent waves (Shrira, Badulin & Kharif 1996; Craig 2001), or via long-wave models like the Benney–Luke and Kadomtsev–Petviashvili equations with a focus on hexagonal waves (Hammack, Scheffner & Segur 1989; Milewski & Keller 1996). Our Hamiltonian method has been applied to similar asymptotic regimes for three-dimensional waves in various physical contexts, e.g. irrotational gravity waves on deep water (Guyenne *et al.* 2022), hydroelastic waves (Guyenne & Părău 2015), and surface waves interacting with topography (Craig *et al.* 2005) or with internal waves (Craig, Guyenne & Sulem 2015).

Author ORCIDs.
- Philippe Guyenne https://orcid.org/0000-0002-4199-3120;
- Adilbek Kairzhan https://orcid.org/0000-0003-1080-1568.

Appendix A. Proof of Lemma 5.3

We provide here the main steps in the proof of Lemma 5.3.

A.1. *Computation of $T_2^{(1)}$*

First, we notice that the terms $S_{(-1-2)12}$, $S_{12(-1-2)}$, $S_{(-3-4)34}$ and $S_{34(-3-4)}$ in (4.15) are of order $O(\varepsilon^2)$. Indeed, under the modulational ansatz (5.1), we have

$$S_{(-1-2)12} = \frac{1 - \text{sgn}(k_1 + k_2)\,\text{sgn}(k_2)}{a_1 a_2 a_{1+2}} \left(-(k_1+k_2)k_2 a_{1+2}^2 a_2^2 - \frac{\gamma}{2} k_1 a_1^2\right) = O(\varepsilon^2), \tag{A1}$$

where, from (5.4), we have $1 - \text{sgn}(k_1 + k_2)\,\text{sgn}(k_2) = O(\varepsilon^2)$ and $a_1, a_2, a_{1+2} = O(1)$. The computations of $S_{12(-1-2)}$, $S_{(-3-4)34}$ and $S_{34(-3-4)}$ are similar. We thus skip such terms as we approximate $T_2^{(1)}$ up to order $O(\varepsilon)$ only. By contrast, the terms $S_{2(-1-2)1}$ and $S_{4(-3-4)3}$ are of order $O(1)$, and they both contribute to the $O(\varepsilon)$ expansion of $T_2^{(1)}$. For the expansion of $S_{2(-1-2)1}$, we use (5.4) and obtain

$$S_{2(-1-2)1} = \frac{(2k_0)^{3/2}(2\omega_0^2 + \gamma\omega_{2k_0})}{2\omega_0\sqrt{\omega_{2k_0}}}$$
$$\times \left[1 - \frac{\varepsilon g}{4}\left(\frac{1}{\omega_0^2} + \frac{1}{\omega_{2k_0}^2} - \frac{3}{gk_0}\right)(\lambda_1+\lambda_2) + \frac{\varepsilon g \Omega_{2k_0}}{\omega_{2k_0}(2\omega_0^2 + \gamma\omega_{2k_0})}(\lambda_1+\lambda_2)\right], \tag{A2}$$

with a similar expression for $S_{4(-3-4)3}$ where $(\lambda_1 + \lambda_2)$ is replaced by $(\lambda_3 + \lambda_4)$. It remains to get an expansion for the bracket on the second line of (4.15). Using (5.4), we have

$$\frac{1}{\Omega_1 + \Omega_2 + \Omega_{-1-2}} + \frac{1}{\Omega_3 + \Omega_4 + \Omega_{-3-4}}$$

$$= \frac{2}{2\Omega_0 + \Omega_{-2k_0}} \left(1 - \frac{\varepsilon g(\omega_0 + \omega_{2k_0})}{4\omega_0 \omega_{2k_0}(2\Omega_0 + \Omega_{-2k_0})} (\lambda_1 + \lambda_2 + \lambda_3 + \lambda_4) \right). \tag{A3}$$

We substitute the above estimates into the expression (4.15) for $T_2^{(1)}$, and use that

$$\int (\lambda_1 + \lambda_2 + \lambda_3 + \lambda_4) z_1 z_2 \bar{z}_3 \bar{z}_4 \, \delta_{1+2-3-4} \, dk_{1234} = 2 \int (\lambda_2 + \lambda_3) z_1 z_2 \bar{z}_3 \bar{z}_4 \, \delta_{1+2-3-4} \, dk_{1234}, \tag{A4}$$

to get

$$\int T_2^{(1)} z_1 z_2 \bar{z}_3 \bar{z}_4 \, \delta_{1+2-3-4} \, dk_{1234}$$

$$= \int \left(c_1^l + \varepsilon c_1^r (\lambda_2 + \lambda_3) \right) z_1 z_2 \bar{z}_3 \bar{z}_4 \, \delta_{1+2-3-4} \, dk_{1234} + O(\varepsilon^2), \tag{A5}$$

which identifies to (5.13) in terms of the variable U. A similar calculation is performed for $T_2^{(2)}$.

A.2. *Computation of $T_2^{(3)}$*

We estimate each term in (4.17) under the modulational ansatz (5.1). Due to dependence on $(k_1 - k_3)$, these terms are of different orders compared to the above computations for $T_2^{(1)}$. Indeed, we show that $A_{(1-3)(-1)3}$ and $A_{(4-2)(-4)2}$ are of order $O(\varepsilon^{1/2})$, and the bracket in (4.17) is of order $O(\varepsilon^{-1})$.

We start with $A_{(1-3)(-1)3}$. Using (3.21*a*,*b*), we need to compute $S_{(1-3)(-1)3}$, $S_{3(1-3)(-1)}$ and $S_{(-1)3(1-3)}$. We immediately rule out the contribution from $S_{3(1-3)(-1)}$ as it is of order $O(\varepsilon^{5/2})$. The remaining terms are combined using (3.21*a*,*b*) as follows:

$$S_{(1-3)(-1)3} - S_{(-1)3(1-3)} = \frac{1}{a_1 a_3 a_{1-3}} \left(\omega_{1-3}(\omega_3 - \omega_1) + \frac{\gamma}{2} \operatorname{sgn}(k_1 - k_3)(\omega_1 - \omega_3) \right.$$

$$\left. + \frac{\gamma}{2}(\omega_1 + \omega_3) + \operatorname{sgn}(k_1 - k_3)\omega_{1-3}(\omega_1 + \omega_3) \right). \tag{A6}$$

Using expansions (5.4), we obtain

$$S_{(1-3)(-1)3} - S_{(-1)3(1-3)}$$

$$= \frac{\sqrt{2} k_0 \varepsilon^{1/2} |\lambda_1 - \lambda_3|^{1/2}}{\sqrt{|\gamma|}\,\omega_0} \left[1 - \frac{\varepsilon}{4} \left(\frac{g}{\omega_0^2} - \frac{2}{k_0} \right) (\lambda_1 + \lambda_3) - \frac{g}{\gamma^2} \varepsilon |\lambda_1 - \lambda_3| \right]$$

$$\times \left[|\gamma|\,\omega_0(\operatorname{sgn}(\gamma) + \operatorname{sgn}(k_1 - k_3)) + \frac{\varepsilon g |\gamma|}{4\omega_0} (\operatorname{sgn}(\gamma) + \operatorname{sgn}(k_1 - k_3))(\lambda_1 + \lambda_3) \right.$$

$$\left. + \frac{\varepsilon g \gamma}{4\omega_0} (\operatorname{sgn}(k_1 - k_3) - \operatorname{sgn}(\gamma))(\lambda_1 - \lambda_3) + \frac{2\varepsilon g \omega_0}{|\gamma|} (\lambda_1 - \lambda_3) \right], \tag{A7}$$

and a similar expression for $A_{(4-2)(-4)2}$ with (k_1, k_3) replaced by (k_4, k_2). Furthermore, using that $(\mathrm{sgn}(k_1 - k_3) + \mathrm{sgn}(\gamma))(\mathrm{sgn}(k_1 - k_3) - \mathrm{sgn}(\gamma)) = 0$, several terms in the product $A_{(1-3)(-1)3}A_{(4-2)(-4)2}$ vanish, and

$$
\begin{aligned}
&A_{(1-3)(-1)3}\, A_{(4-2)(-4)2} \\
&= \frac{\varepsilon k_0^2 \gamma (\lambda_1 - \lambda_3)}{16\pi} \left(1 + \mathrm{sgn}(\gamma)\, \mathrm{sgn}(k_1 - k_3)\right) \left(1 + \frac{\varepsilon}{2k_0}\left(\lambda_1 + \lambda_2 + \lambda_3 + \lambda_4\right)\right) + O(\varepsilon^3).
\end{aligned}
\tag{A8}
$$

In addition, for (4.17), we have

$$
\begin{aligned}
&\frac{1}{\Omega_{3-1} + \Omega_1 - \Omega_3} + \frac{1}{\Omega_{2-4} + \Omega_4 - \Omega_2} \\
&= \frac{2\gamma \omega_0}{\varepsilon(\lambda_1 - \lambda_3)g\Omega_0} \left(1 + \frac{\varepsilon g \gamma}{16\omega_0^2 \Omega_0}\left(\lambda_1 + \lambda_2 + \lambda_3 + \lambda_4\right) + \frac{\varepsilon g \omega_0}{\gamma^2 \Omega_0}|\lambda_1 - \lambda_3|\right).
\end{aligned}
\tag{A9}
$$

We combine these estimates according to (4.17), and (5.13) follows.

REFERENCES

BAUMSTEIN, A.I. 1998 Modulation of gravity waves with shear in water. *Stud. Appl. Maths* **100**, 365–390.

BENJAMIN, T.B. & OLVER, P.J. 1982 Hamiltonian structure, symmetries and conservation laws for water waves. *J. Fluid Mech.* **125**, 137–185.

BERTI, M., FRANZOI, L. & MASPERO, A. 2021 Traveling quasi-periodic water waves with constant vorticity. *Arch. Rat. Mech. Anal.* **240**, 99–202.

BLYTH, M.G. & PĂRĂU, E.I. 2022 Stability of waves on fluid of infinite depth with constant vorticity. *J. Fluid Mech.* **936**, A46.

CASTRO, A. & LANNES, D. 2014 Fully nonlinear long-wave models in the presence of vorticity. *J. Fluid Mech.* **759**, 642–675.

CHOI, W. 2009 Nonlinear surface waves interacting with a linear shear current. *Maths Comput. Simul.* **80**, 29–36.

COIFMAN, R. & MEYER, Y. 1985 Nonlinear harmonic analysis and analytic dependence. *Proc. Symp. Pure Maths* **43**, 71–78.

CONSTANTIN, A. 2001 *Nonlinear Water Waves with Applications to Wave–Current Interactions and Tsunamis.* CBMS-NSF Regional Conference Series in Applied Mathematics, vol. 81. SIAM.

CONSTANTIN, A., IVANOV, R.I. & PRODANOV, E.M. 2008 Nearly-Hamiltonian structure for water waves with constant vorticity. *J. Math. Fluid Mech.* **10**, 224–237.

CRAIG, W. 2001 On the Badulin, Kharif and Shrira model of resonant water waves. *Physica* D **152–153**, 434–450.

CRAIG, W., GUYENNE, P., NICHOLLS, D.P. & SULEM, C. 2005 Hamiltonian long-wave expansions for water waves over a rough bottom. *Proc. R. Soc. Lond.* A **461**, 839–873.

CRAIG, W., GUYENNE, P. & SULEM, C. 2010 A Hamiltonian approach to nonlinear modulation of surface water waves. *Wave Motion* **47**, 552–563.

CRAIG, W., GUYENNE, P. & SULEM, C. 2015 Internal waves coupled to surface gravity waves in three dimensions. *Commun. Math. Sci.* **13**, 893–910.

CRAIG, W., GUYENNE, P. & SULEM, C. 2021*a* Normal form transformations and Dysthe's equation for the nonlinear modulation of deep-water gravity waves. *Water Waves* **3**, 127–152.

CRAIG, W., GUYENNE, P. & SULEM, C. 2021*b* The water wave problem and Hamiltonian transformation theory. In *Waves in Flows* (ed. T. Bodnár, G. Galdi, & Š. Nečasová), Adv. Math. Fluid Mech., pp. 113–196. Birkhäuser.

CRAIG, W. & SULEM, C. 1993 Numerical simulations of gravity waves. *J. Comput. Phys.* **108**, 73–83.

CRAIG, W. & SULEM, C. 2016 Mapping properties of normal forms transformations for water waves. *Boll. Unione Mat. Ital.* **9**, 289–318.

CURTIS, C.W., CARTER, J.D. & KALISCH, H. 2018 Particle paths in nonlinear Schrödinger models in the presence of linear shear currents. *J. Fluid Mech.* **855**, 322–350.

949 A50-38

CURTIS, C.W. & MURPHY, M. 2020 Evolution of spectral distribution in deep-water constant vorticity flows. *Water Waves* **2**, 361–380.

DYACHENKO, S.A. & HUR, V.M. 2019 Stokes waves with constant vorticity: folds, gaps and fluid bubbles. *J. Fluid Mech.* **878**, 502–521.

DYSTHE, K.B. 1979 Note on a modification to the nonlinear Schrödinger equation for application to deep water waves. *Proc. R. Soc. Lond.* A **369**, 105–114.

GAO, T., WANG, Z. & MILEWSKI, P.A. 2019 Nonlinear hydroelastic waves on a linear shear current at finite depth. *J. Fluid Mech.* **876**, 55–86.

GRAMSTAD, O. & TRULSEN, K. 2011 Hamiltonian form of the modified nonlinear Schrödinger equation for gravity waves on arbitrary depth. *J. Fluid Mech.* **670**, 404–426.

GUYENNE, P. 2017 A high-order spectral method for nonlinear water waves in the presence of a linear shear current. *Comput. Fluids* **154**, 224–235.

GUYENNE, P. 2018 A high-order spectral method for a vertical 2D model of nonlinear water waves interacting with a linear shear current. In *Proceedings of the 28th International Ocean Polar Engng Conference (ISOPE 2018), Sapporo, Japan, June 10–15* (ed. J.S. Chung, B.-S, Hyun, D. Matskevitch & A.M. Wang), pp. 436–443. ISOPE.

GUYENNE, P., KAIRZHAN, A. & SULEM, C. 2022 Hamiltonian Dysthe equation for three-dimensional deep-water gravity waves. *Multiscale Model. Simul.* **20**, 349–378.

GUYENNE, P., KAIRZHAN, A., SULEM, C. & XU, B. 2021 Spatial form of a Hamiltonian Dysthe equation for deep-water gravity waves. *Fluids* **6**, 103.

GUYENNE, P. & PĂRĂU, E.I. 2015 Asymptotic modeling and numerical simulation of solitary waves in a floating ice sheet. In *Proceedings of the 25th International Ocean Polar Engng Conference (ISOPE 2015), Kona, Big Island, Hawaii, USA, June 21–26* (ed. J.S. Chung, F. Vorpahl, S. Young Hong, T. Kokkinis & A.M. Wang), pp. 467–475. ISOPE.

HAMMACK, J., SCHEFFNER, N. & SEGUR, H. 1989 Two-dimensional periodic waves in shallow water. *J. Fluid Mech.* **209**, 567–589.

HSU, H.C., KHARIF, C., ABID, M. & CHEN, Y.Y. 2018 A nonlinear Schrödinger equation for gravity–capillary water waves on arbitrary depth with constant vorticity. *J. Fluid Mech.* **854**, 146–163.

HUR, V.M. & WHEELER, M.H. 2020 Exact free surfaces in constant vorticity flows. *J. Fluid Mech.* **896**, R1.

KRASITSKII, V.P. 1994 On reduced equations in the Hamiltonian theory of weakly nonlinear surface waves. *J. Fluid Mech.* **272**, 1–20.

LANNES, D. 2013 *The Water Waves Problem: Mathematical Analysis and Asymptotics*. Mathematical Surveys and Monographs, vol. 188. AMS.

LO, E. & MEI, C.C. 1985 A numerical study of water-wave modulation based on a higher-order nonlinear Schrödinger equation. *J. Fluid Mech.* **150**, 395–416.

MILEWSKI, P.A. & KELLER, J.B. 1996 Three-dimensional water waves. *Stud. Appl. Maths* **37**, 149–166.

MOREIRA, R.M. & CHACALTANA, J.T.A. 2015 Vorticity effects on nonlinear wave–current interactions in deep water. *J. Fluid Mech.* **778**, 314–334.

OBRECHT, C. & SAUT, J.-C. 2015 Remarks on the full dispersion Davey–Stewartson systems. *Commun. Pure Appl. Anal.* **14**, 1547–1561.

RIBEIRO, R. JR., MILEWSKI, P.A. & NACHBIN, A. 2017 Flow structure beneath rotational water waves with stagnation points. *J. Fluid Mech.* **812**, 792–814.

RICHARD, G.L. & GAVRILYUK, S.L. 2015 Modelling turbulence generation in solitary waves on shear shallow water flows. *J. Fluid Mech.* **773**, 49–74.

SEGAL, B.L., MOLDABAYEV, D., KALISCH, H. & DECONINCK, B. 2017 Explicit solutions for a long-wave model with constant vorticity. *Eur. J. Mech. (B/Fluids)* **65**, 247–256.

SHRIRA, V.I., BADULIN, S.I. & KHARIF, C. 1996 A model of water wave 'horse-shoe' patterns. *J. Fluid Mech.* **318**, 375–405.

STEER, J.N., BORTHWICK, A.G.L., STAGONAS, D., BULDAKOV, E. & VAN DEN BREMER, T.S. 2019 Experimental study of dispersion and modulational instability of surface gravity waves on constant vorticity currents. *J. Fluid Mech.* **884**, A40.

TELES DA SILVA, A.F. & PEREGRINE, D.H. 1988 Steep, steady surface waves on water of finite depth with constant vorticity. *J. Fluid Mech.* **195**, 281–302.

THOMAS, R., KHARIF, C. & MANNA, M. 2012 A nonlinear Schrödinger equation for water waves on finite depth with constant vorticity. *Phys. Fluids* **24**, 127102.

TRULSEN, K., KLIAKHANDLER, I., DYSTHE, K.B. & VELARDE, M.G. 2000 On weakly nonlinear modulation of waves on deep water. *Phys. Fluids* **12**, 2432–2437.

VANDEN-BROECK, J.-M. 1996 Periodic waves with constant vorticity in water of infinite depth. *IMA J. Appl. Maths* **56**, 207–217.

WAHLÉN, E. 2007 A Hamiltonian formulation of water waves with constant vorticity. *Lett. Math. Phys.* **79**, 303–315.

WAHLÉN, E. 2008 Hamiltonian long-wave approximations of water waves with constant vorticity. *Phys. Lett. A* **372**, 2597–2602.

XU, L. & GUYENNE, P. 2009 Numerical simulation of three-dimensional nonlinear water waves. *J. Comput. Phys.* **228**, 8446–8466.

ZAKHAROV, V.E. 1968 Stability of periodic waves of finite amplitude on the surface of a deep fluid. *J. Appl. Mech. Tech. Phys.* **9**, 190–194.

ZHANG, H.D., GUEDES SOARES, C. & ONORATO, M. 2015 Modelling of the spatial evolution of extreme laboratory wave crest and trough heights with the NLS-type equations. *Appl. Ocean Res.* **52**, 140–150.